
Splitting Steepest Descent for Growing Neural Architectures

Qiang Liu
UT Austin
lqiang@cs.utexas.edu

Lemeng Wu *
UT Austin
lmwu@cs.utexas.edu

Dilin Wang *
UT Austin
dilin@cs.utexas.edu

Abstract

We develop a progressive training approach for neural networks which adaptively grows the network structure by splitting existing neurons to multiple off-springs. By leveraging a functional steepest descent idea, we derive a simple criterion for deciding the best subset of neurons to split and a *splitting gradient* for optimally updating the off-springs. Theoretically, our splitting strategy is a second-order functional steepest descent for escaping saddle points in an ∞ -Wasserstein metric space, on which the standard parametric gradient descent is a first-order steepest descent. Our method provides a new practical approach for optimizing neural network structures, especially for learning lightweight neural architectures in resource-constrained settings.

1 Introduction

Deep neural networks (DNNs) have achieved remarkable empirical successes recently. However, efficient and automatic optimization of model architectures remains to be a key challenge. Compared with parameter optimization which has been well addressed by gradient-based methods (a.k.a. back-propagation), optimizing model structures involves significantly more challenging discrete optimization with large search spaces and high evaluation cost. Although there have been rapid progresses recently, designing the best architectures still requires a lot of expert knowledge and trial-and-errors for most practical tasks.

This work targets extending the power of gradient descent to the domain of model structure optimization of neural networks. In particular, we consider the problem of progressively growing a neural network by “splitting” existing neurons into several “off-springs”, and develop a simple and practical approach for deciding the best subset of neurons to split and how to split them, adaptively based on the existing model structure. We derive the optimal splitting strategies by considering the *steepest descent* of the loss when the off-springs are infinitesimally close to the original neurons, yielding a *splitting steepest descent* that monotonically decreases the loss in the space of model structures.

Our main method, shown in Algorithm 1, alternates between a standard *parametric descent phase* in which we update the parameters to minimize the loss with a fixed model structure, and a *splitting phase* in which we update the model structures by splitting neurons. The splitting phase is triggered when no further improvement can be made by only updating parameters, and allow us to escape the parametric local optima by augmenting the neural network in a locally optimal fashion. Theoretically, these two phases can be viewed as performing functional steepest descent on an ∞ -Wasserstein metric space, in which the splitting phase is a *second-order descent* for escaping saddle points in the functional space, while the parametric gradient descent corresponds to a *first-order descent*. Empirically, our algorithm is simple and practical, and provides a promising tool for many challenging problems, especially for learning lightweight and energy-efficient neural architectures for resource-constrained settings.

*equal contribution

Related Works The idea of progressively growing neural networks by node splitting is not new, but previous works are mostly based on heuristic or purely random splitting strategies (e.g., Wynne-Jones, 1992; Chen et al., 2016). A different approach for progressive training is the Frank-Wolfe or gradient boosting based strategies (e.g., Schwenk & Bengio, 2000; Bengio et al., 2006; Bach, 2017), which iteratively add new neurons derived from functional conditional gradient, while keeping the previous neurons fixed. However, these methods are not suitable for large scale settings, because adding each neuron requires to solve a difficult non-convex optimization problem, and keeping the previous neurons fixed prevents us from correcting the mistakes made in earlier iterations. A practical alternative of Frank-Wolfe is to simply add new randomly initialized neurons and co-optimize the new and old neurons together. However, random initialization does not allow us to leverage the information of the existing model and takes more time to converge. In contrast, splitting neurons from the existing network allows us to inherit the knowledge from the existing model (see Chen et al. (2016)), and is faster to converge in settings like continual learning, when the previous model is not far away from the optimal solution.

An opposite direction of progressive training is to *prune* large pre-trained neural networks to obtain compact network structures (e.g., Han et al., 2016; Li et al., 2017; Liu et al., 2017). In comparison, our splitting method requires no large pre-trained models and is more suitable for learning *very small* network structures, which is of critical importance for resource-constrained settings like mobile devices and Internet of things. As shown in our experiments, our method can outperform existing pruning methods in learning more accurate models with small model sizes.

More broadly, there has been a series of recent works on neural architecture search, based on various strategies from combinatorial optimization, including reinforcement learning (RL) (e.g., Pham et al., 2018; Cai et al., 2018; Zoph & Le, 2017), evolutionary algorithms (EA) (e.g., Stanley & Miikkulainen, 2002; Real et al., 2018), and continuous relaxation (e.g., Liu et al., 2019a; Xie et al., 2018). However, these general-purpose black-box optimization methods do not efficiently leverage the inherent geometric structure of the loss landscape, and are highly computationally expensive due to the need of evaluating the candidate architectures based on inner training loops.

Background: Steepest Descent and Saddle Points Stochastic gradient descent is the driving horse for solving large scale optimization in machine learning and deep learning. Gradient descent can be viewed as a steepest descent procedure that iteratively improves the solution by following the direction that maximally decreases the loss function within a small neighborhood of the previous solution. Specifically, for minimizing a loss function $L(\theta)$, each iteration of steepest descent updates the parameter via $\theta \leftarrow \theta + \epsilon\delta$, where ϵ is a small step size and δ is an update direction chosen to maximally decrease the loss $L(\theta + \epsilon\delta)$ of the updated parameter under a norm constraint $\|\delta\| \leq 1$, where $\|\cdot\|$ denotes the Euclidean norm. When $\nabla L(\theta) \neq 0$ and ϵ is infinitesimal, the optimal descent direction δ equals the negative gradient direction, that is, $\delta = -\nabla L(\theta) / \|\nabla L(\theta)\|$, yielding a descent of $L(\theta + \epsilon\delta) - L(\theta) \approx -\epsilon \|\nabla L(\theta)\|$. At a critical point with a zero gradient ($\nabla L(\theta) = 0$), the steepest descent direction depends on the spectrum of the Hessian matrix $\nabla^2 L(\theta)$. Denote by λ_{min} the minimum eigenvalue of $\nabla^2 L(\theta)$ and v_{min} its associated eigenvector. When $\lambda_{min} > 0$, the point θ is a stable local minimum and no further improvement can be made in the infinitesimal neighborhood. When $\lambda_{min} < 0$, the point θ is a saddle point or local maximum, and the steepest descent direction equals the eigenvector $\pm v_{min}$, which yields an $\epsilon^2 \lambda_{min} / 2$ decrease on the loss.² In practice, it has been shown that there is no need to explicitly calculate the negative eigenvalue direction, because saddle points and local maxima are unstable and can be escaped by using gradient descent with random initialization or stochastic noise (e.g., Lee et al., 2016; Jin et al., 2017).

2 Splitting Neurons Using Steepest Descent

We introduce our main method in this section. We first illustrate the idea with the simple case of splitting a single neuron in Section 2.1, and then consider the more general case of simultaneously splitting multiple neurons in deep networks in Section 2.2, which yields our main progressive training algorithm (Algorithm 1). Section 2.3 draws a theoretical discussion and interpret our procedure as a functional steepest descent of the distribution of the neuron weights under the ∞ -Wasserstein metric.

²The property of the case when $\lambda_{min} = 0$ depends on higher order information.

2.1 Splitting a Single Neuron

Let $\sigma(\theta, x)$ be a neuron inside a neural network that we want to learn from data, where θ is the parameter of the neuron and x its input variable. Assume the loss of θ has a general form of

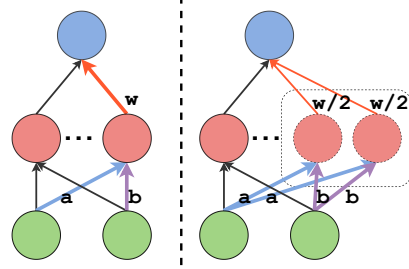
$$L(\theta) := \mathbb{E}_{x \sim \mathcal{D}}[\Phi(\sigma(\theta, x))], \quad (1)$$

where \mathcal{D} is a data distribution, and Φ is a map determined by the overall loss function. The parameters of the other parts of the network are assumed to be fixed or optimized using standard procedures and are omitted for notation convenience.

Standard gradient descent can only yield parametric updates of θ . We introduce a generalized steepest descent procedure that allows us to incrementally grow the neural network by gradually introducing new neurons, achieved by “splitting” the existing neurons into multiple copies in a (locally) optimal fashion derived using ideas from steepest descent idea.

In particular, we split θ into m off-springs $\boldsymbol{\theta} := \{\theta_i\}_{i=1}^m$, and replace the neuron $\sigma(\theta, x)$ with a weighted sum of the off-spring neurons $\sum_{i=1}^m w_i \sigma(\theta_i, x)$, where $\mathbf{w} := \{w_i\}_{i=1}^m$ is a set of positive weights assigned on the off-springs, and satisfies $\sum_{i=1}^m w_i = 1, w_i > 0$. This yields an augmented loss function on $\boldsymbol{\theta}$ and \mathbf{w} :

$$\mathcal{L}(\boldsymbol{\theta}, \mathbf{w}) := \mathbb{E}_{x \sim \mathcal{D}} \left[\Phi \left(\sum_{i=1}^m w_i \sigma(\theta_i, x) \right) \right]. \quad (2)$$



A key property of this construction is that it introduces a smooth change on the loss function when the off-springs $\{\theta_i\}_{i=1}^m$ are close to the original parameter θ : when $\theta_i = \theta, \forall i = 1, \dots, m$, the augmented network and loss are equivalent to the original ones, that is, $\mathcal{L}(\theta \mathbf{1}_m, \mathbf{w}) = L(\theta)$, where $\mathbf{1}_m$ denotes the $m \times 1$ vector consisting of all ones; when all the $\{\theta_i\}$ are within an infinitesimal neighborhood of θ , it yields an infinitesimal change on the loss, with which a steepest descent can be derive.

Formally, consider the set of splitting schemes $(m, \boldsymbol{\theta}, \mathbf{w})$ whose off-springs are ϵ -close to the original neuron:

$$\{(m, \boldsymbol{\theta}, \mathbf{w}) : m \in \mathbb{N}_+, \|\theta_i - \theta\| \leq \epsilon, \sum_{i=1}^m w_i = 1, w_i > 0, \forall i = 1, \dots, m\}.$$

We want to decide the optimal $(m, \boldsymbol{\theta}, \mathbf{w})$ to maximize the decrease of loss $\mathcal{L}(\boldsymbol{\theta}, \mathbf{w}) - L(\theta)$, when the step size ϵ is infinitesimal. Although this appears to be an infinite dimensional optimization because m is allowed to be arbitrarily large, we show that the optimal choice is achieved with either $m = 1$ (no splitting) or $m = 2$ (splitting into two off-springs), with uniform weights $w_i = 1/m$. Whether a neuron should be split ($m = 1$ or 2) and the optimal values of the off-springs $\{\theta_i\}$ are decided by the minimum eigenvalue and eigenvector of a *splitting matrix*, which plays a role similar to Hessian matrix for deciding saddle points.

Definition 2.1 (Splitting Matrix). For $L(\theta)$ in (1), its *splitting matrix* $S(\theta)$ is defined as

$$S(\theta) = \mathbb{E}_{x \sim \mathcal{D}}[\Phi'(\sigma(\theta, x)) \nabla_{\theta\theta}^2 \sigma(\theta, x)]. \quad (3)$$

We call the minimum eigenvalue $\lambda_{\min}(S(\theta))$ of $S(\theta)$ the *splitting index* of θ , and the eigenvector $v_{\min}(S(\theta))$ related to $\lambda_{\min}(S(\theta))$ the *splitting gradient* of θ .

The splitting matrix $S(\theta)$ is a $\mathbb{R}^{d \times d}$ symmetric “semi-Hessian” matrix that involves the first derivative $\Phi'(\cdot)$, and the second derivative of $\sigma(\theta, x)$. It is useful to compare it with the typical gradient and Hessian matrix of $L(\theta)$:

$$\nabla_{\theta} L(\theta) = \mathbb{E}_{x \sim \mathcal{D}}[\Phi'(\sigma(\theta, x)) \nabla_{\theta} \sigma(\theta, x)], \quad \nabla_{\theta\theta}^2 L(\theta) = S(\theta) + \underbrace{\mathbb{E}[\Phi''(\sigma(\theta, x)) \nabla_{\theta} \sigma(\theta, x)^{\otimes 2}]}_{T(\theta)},$$

where $v^{\otimes 2} := vv^{\top}$ is the outer product. The splitting matrix $S(\theta)$ differs from the gradient $\nabla_{\theta} L(\theta)$ in replacing $\nabla_{\theta} \sigma(\theta, x)$ with the second-order derivative $\nabla_{\theta\theta}^2 \sigma(\theta, x)$, and differs from the Hessian

matrix $\nabla_{\theta\theta}^2 L(\theta)$ in missing an extra term $T(\theta)$. We should point out that $S(\theta)$ is the “easier part” of the Hessian matrix, because the second-order derivative $\nabla_{\theta\theta}^2 \sigma(\theta, x)$ of the individual neuron σ is much simpler than the second-order derivative $\Phi''(\cdot)$ of “everything else”, which appears in the extra term $T(\theta)$. In addition, as we show in Section 2.2, $S(\theta)$ is block diagonal in terms of multiple neurons, which is crucial for enabling practical computational algorithm.

It is useful to decompose each θ_i into $\theta_i = \theta + \epsilon(\mu + \delta_i)$, where μ is an average displacement vector shared by all copies, and δ_i is the splitting vector associated with θ_i , and satisfies $\sum_i w_i \delta_i = 0$ (which implies $\sum_i w_i \theta_i = \theta + \epsilon\mu$). It turns out that the change of loss $\mathcal{L}(\boldsymbol{\theta}, \mathbf{w}) - L(\theta)$ naturally decomposes into two terms that reflect the effects of the average displacement and splitting, respectively.

Theorem 2.2. *Assume $\theta_i = \theta + \epsilon(\mu + \delta_i)$ with $\sum_i w_i \delta_i = 0$ and $\sum_i w_i = 1$. For $L(\theta)$ and $\mathcal{L}(\boldsymbol{\theta}, \mathbf{w})$ in (1) and (2), assume $\mathcal{L}(\boldsymbol{\theta}, \mathbf{w})$ has bounded third order derivatives w.r.t. $\boldsymbol{\theta}$. We have*

$$\mathcal{L}(\boldsymbol{\theta}, \mathbf{w}) - L(\theta) = \underbrace{\epsilon \nabla L(\theta)^\top \mu + \frac{\epsilon^2}{2} \mu^\top \nabla^2 L(\theta) \mu}_{I(\mu; \theta) = L(\theta + \epsilon\mu) - L(\theta) + \mathcal{O}(\epsilon^3)} + \underbrace{\frac{\epsilon^2}{2} \sum_{i=1}^m w_i \delta_i^\top S(\theta) \delta_i}_{II(\boldsymbol{\delta}, \mathbf{w}; \theta)} + \mathcal{O}(\epsilon^3), \quad (4)$$

where the change of loss is decomposed into two terms: the first term $I(\mu; \theta)$ is the effect of the average displacement μ , and it is equivalent to applying the standard parametric update $\theta \leftarrow \theta + \epsilon\mu$ on $L(\theta)$. The second term $II(\boldsymbol{\delta}, \mathbf{w}; \theta)$ is the change of the loss caused by the splitting vectors $\boldsymbol{\delta} := \{\delta_i\}$. It depends on $L(\theta)$ only through the splitting matrix $S(\theta)$.

Therefore, the optimal average displacement μ should be decided by standard parametric steepest (gradient) descent, which yields a typical $\mathcal{O}(\epsilon)$ decrease of loss at non-stationary points. In comparison, the splitting term $II(\boldsymbol{\delta}, \mathbf{w}; \theta)$ is always $\mathcal{O}(\epsilon^2)$, which is much smaller. Given that introducing new neurons increases model size, splitting should not be preferred unless it is impossible to achieve an $\mathcal{O}(\epsilon^2)$ gain with pure parametric updates that do not increase the model size. Therefore, it is motivated to introduce splitting only at stable local minima, when the optimal μ equals zero and no further improvement is possible with (infinitesimal) regular parametric descent on $L(\theta)$. In this case, we only need to minimize the splitting term $II(\boldsymbol{\delta}, \mathbf{w}; \theta)$ to decide the optimal splitting strategy, which is shown in the following theorem.

Theorem 2.3. *a) If the splitting matrix is positive definite, that is, $\lambda_{\min}(S(\theta)) > 0$, we have $II(\boldsymbol{\delta}, \mathbf{w}; \theta) > 0$ for any $\mathbf{w} > 0$ and $\boldsymbol{\delta} \neq 0$, and hence no infinitesimal splitting can decrease the loss. We call that θ is splitting stable in this case.*

b) If $\lambda_{\min}(S(\theta)) < 0$, an optimal splitting strategy that minimizes $II(\boldsymbol{\delta}, \mathbf{w}; \theta)$ subject to $\|\delta_i\| \leq 1$ is

$$m = 2, \quad w_1 = w_2 = 1/2, \quad \text{and} \quad \delta_1 = v_{\min}(S(\theta)), \quad \delta_2 = -v_{\min}(S(\theta)),$$

where $v_{\min}(S(\theta))$, called the splitting gradient, is the eigenvector related to $\lambda_{\min}(S(\theta))$. Here we split the neuron into two copies of equal weights, and update each copy with the splitting gradient. The change of loss obtained in this case is $II(\{\delta_1, -\delta_1\}, \{1/2, 1/2\}; \theta) = -\epsilon^2 \lambda_{\min}(S(\theta))/2 < 0$.

Remark The splitting stability ($S(\theta) \succ 0$) does not necessarily ensure the standard parametric stability of $L(\theta)$ (i.e., $\nabla^2 L(\theta) = S(\theta) + T(\theta) \succ 0$), except when $\Phi(\cdot)$ is convex which ensures $T(\theta) \succeq 0$ (see Definition 2.1). If both $S(\theta) \succ 0$ and $\nabla^2 L(\theta) \succ 0$ hold, the loss can not be improved by any local update or splitting, no matter how many off-springs are allowed. Since stochastic gradient descent guarantees to escape unstable stationary points (Lee et al., 2016; Jin et al., 2017), we only need to calculate $S(\theta)$ to decide the splitting stability in practice.

2.2 Splitting Deep Neural Networks

In practice, we need to split multiple neurons simultaneously, which may be of different types, or locate in different layers of a deep neural network. The key questions are if the optimal splitting strategies of different neurons influence each other in some way, and how to compare the gain of splitting different neurons and select the best subset of neurons to split under a budget constraint.

It turns out the answers are simple. We show that the change of loss caused by splitting a set of neurons is simply the sum of the splitting terms $II(\boldsymbol{\delta}, \mathbf{w}; \theta)$ of the individual neurons. Therefore, we

Algorithm 1 Splitting Steepest Descent for Optimizing Neural Architectures

Initialize a neural network with a set of neurons $\theta^{[1:n]} = \{\theta^{[\ell]}\}_{\ell=1}^n$ that can be split, whose loss satisfies (5). Decide a maximum number m_* of neurons to split at each iteration, and a threshold $\lambda_* \leq 0$ of the splitting index. A stepsize ϵ .

1. Update the parameters using standard optimizers (e.g., stochastic gradient descent) until no further improvement can be made by only updating parameters.

2. Calculate the splitting matrices $\{S^{[\ell]}\}$ of the neurons following (7), as well as their minimum eigenvalues $\{\lambda_{min}^{[\ell]}\}$ and the associated eigenvectors $\{v_{min}^{[\ell]}\}$.

3. Select the set of neurons to split by picking the top m_* neurons with the smallest eigenvalues $\{\lambda_{min}^{[\ell]}\}$ and satisfies $\lambda_{min}^{[\ell]} \leq \lambda_*$.

4. Split each of the selected neurons into two off-springs with equal weights, and update the neuron network by replacing each selected neuron $\sigma_\ell(\theta^{[\ell]}, \cdot)$ with

$$\frac{1}{2}(\sigma_\ell(\theta_1^{[\ell]}, \cdot) + \sigma_\ell(\theta_2^{[\ell]}, \cdot)), \quad \text{where} \quad \theta_1^{[\ell]} \leftarrow \theta^{[\ell]} + \epsilon v_{min}^{[\ell]}, \quad \theta_2^{[\ell]} \leftarrow \theta^{[\ell]} - \epsilon v_{min}^{[\ell]}.$$

Update the list of neurons. Go back to Step 1 or stop when a stopping criterion is met.

can calculate the splitting matrix of each neuron independently without considering the other neurons, and compare the “splitting desirability” of the different neurons by their minimum eigenvalues (splitting indexes). This motivates our main algorithm (Algorithm 1), in which we progressively split the neurons with the most negative splitting indexes following their own splitting gradients. Since the neurons can be in different layers and of different types, this provides an adaptive way to grow neural network structures to fit best with data.

To set up the notation, let $\theta^{[1:n]} = \{\theta^{[1]}, \dots, \theta^{[n]}\}$ be the parameters of a set of neurons (or any duplicable sub-structures) in a large neural network, where $\theta^{[\ell]}$ is the parameter of the ℓ -th neuron. Assume we split $\theta^{[\ell]}$ into m_ℓ copies $\boldsymbol{\theta}^{[\ell]} := \{\theta_i^{[\ell]}\}_{i=1}^{m_\ell}$, with weights $\boldsymbol{w}^{[\ell]} = \{w_i^{[\ell]}\}_{i=1}^{m_\ell}$ satisfying $\sum_{i=1}^{m_\ell} w_i^{[\ell]} = 1$ and $w_i^{[\ell]} \geq 0, \forall i = 1, \dots, m_\ell$. Denote by $L(\theta^{[1:n]})$ and $\mathcal{L}(\boldsymbol{\theta}^{[1:n]}, \boldsymbol{w}^{[1:n]})$ the loss function of the original and augmented networks, respectively. It is hard to specify the actual expression of the loss functions in general cases, but it is sufficient to know that $L(\theta^{[1:n]})$ depends on each $\theta^{[\ell]}$ only through the output of its related neuron,

$$L(\theta^{[1:n]}) = \mathbb{E}_{x \sim \mathcal{D}} \left[\Phi_\ell \left(\sigma_\ell \left(\theta^{[\ell]}, h^{[\ell]} \right); \theta^{[-\ell]} \right) \right], \quad h^{[\ell]} = g_\ell(x; \theta^{[-\ell]}), \quad (5)$$

where σ_ℓ denotes the activation function of neuron ℓ , and g_ℓ and Φ_ℓ denote the parts of the loss that connect to the input and output of neuron ℓ , respectively, both of which depend on the other parameters $\theta^{[-\ell]}$ in some complex way. Similarly, the augmented loss $\mathcal{L}(\boldsymbol{\theta}^{[1:n]}, \boldsymbol{w}^{[1:n]})$ satisfies

$$\mathcal{L}(\boldsymbol{\theta}^{[1:n]}, \boldsymbol{w}^{[1:n]}) = \mathbb{E}_{x \sim \mathcal{D}} \left[\Phi_\ell \left(\sum_{i=1}^{m_\ell} w_i \sigma_\ell \left(\theta_i^{[\ell]}, \boldsymbol{h}^{[\ell]} \right); \theta^{[-\ell]}, \boldsymbol{w}^{[-\ell]} \right) \right], \quad (6)$$

where $\boldsymbol{h}^{[\ell]} = g_\ell(x; \theta^{[-\ell]}, \boldsymbol{w}^{[-\ell]})$, and $\boldsymbol{g}_\ell, \Phi_\ell$ are the augmented variants of g_ℓ, Φ_ℓ , respectively.

Interestingly, although each equation in (5) and (6) only provides a partial specification of the loss function of deep neural nets, they together are sufficient to establish the following key extension of Theorem 2.2 to the case of multiple neurons.

Theorem 2.4. *Under the setting above, assume $\theta_i^{[\ell]} = \theta^{[\ell]} + \epsilon(\mu^{[\ell]} + \delta_i^{[\ell]})$ for $\forall \ell \in [1:n]$, where $\mu^{[\ell]}$ denotes the average displacement vector on $\theta^{[\ell]}$, and $\delta_i^{[\ell]}$ is the i -th splitting vector of $\theta^{[\ell]}$, with $\sum_{i=1}^{m_\ell} w_i \delta_i^{[\ell]} = 0$. Assume $\mathcal{L}(\boldsymbol{\theta}^{[1:n]}, \boldsymbol{w}^{[1:n]})$ has bounded third order derivatives w.r.t. $\boldsymbol{\theta}^{[1:n]}$. We have*

$$\mathcal{L}(\boldsymbol{\theta}^{[1:n]}, \boldsymbol{w}^{[1:n]}) = L(\theta^{[1:n]} + \epsilon \mu^{[1:n]}) + \underbrace{\sum_{\ell=1}^n \frac{\epsilon^2}{2} \sum_{i=1}^{m_\ell} w_i^{[\ell]} \delta_i^{[\ell]\top} S^{[\ell]}(\theta^{[1:n]}) \delta_i^{[\ell]}}_{H_\ell(\boldsymbol{\delta}^{[\ell]}, \boldsymbol{w}^{[\ell]}; \theta^{[1:n]})} + \mathcal{O}(\epsilon^3),$$

where the effect of average displacement is again equivalent to that of the corresponding parametric update $\theta^{[1:n]} \leftarrow \theta^{[1:n]} + \epsilon \mu^{[1:n]}$; the splitting effect equals the sum of the individual splitting terms $\Pi_\ell(\delta^{[\ell]}, \mathbf{w}^{[\ell]}; \theta^{[1:n]})$, which depends on the splitting matrix $S^{[\ell]}(\theta^{[1:n]})$ of neuron ℓ ,

$$S^{[\ell]}(\theta^{[1:n]}) = \mathbb{E}_{x \sim \mathcal{D}} \left[\nabla_{\sigma_\ell} \Phi_\ell \left(\sigma_\ell \left(\theta^{[\ell]}, h^{[\ell]} \right); \theta^{[-\ell]} \right) \nabla_{\theta\theta}^2 \sigma_\ell \left(\theta^{[\ell]}, h^{[\ell]} \right) \right]. \quad (7)$$

The important implication of Theorem 2.4 is that there is *no crossing term* in the splitting matrix, unlike the standard Hessian matrix. Therefore, the splitting effect of an individual neuron only depends on its own splitting matrix and can be evaluated individually; the splitting effects of different neurons can be compared using their splitting indexes, allowing us to decide the best subset of neurons to split when a maximum number constraint is imposed. As shown in Algorithm 1, we decide a maximum number m_* of neurons to split at each iteration, and a threshold $\lambda_* \leq 0$ of splitting index, and split the neurons whose splitting indexes are ranked in top m_* and smaller than λ_* .

Computational Efficiency The computational cost of exactly evaluating all the splitting indexes and gradients on a data instance is $\mathcal{O}(nd^3)$, where n is the number of neurons and d is the number of the parameters of each neuron. Note that this is much better than evaluating the Hessian matrix, which costs $\mathcal{O}(N^3)$, where N is the total number of parameters (e.g., $N \geq nd$). In practice, d is not excessively large or can be controlled by identifying a subset of important neurons to split. Further computational speedup can be obtained by using efficient gradient-based large scale eigen-computation methods, which we investigate in future work.

2.3 Splitting as ∞ -Wasserstein Steepest Descent

We present a functional aspect of our approach, in which we frame the co-optimization of the neural parameters and structures into a functional optimization in the space of distributions of the neuron weights, and show that our splitting strategy can be viewed as a second-order descent for escaping saddle points in the ∞ -Wasserstein space of distributions, while the standard parametric gradient descent corresponds to a first-order descent in the same space.

We illustrate our theory using the single neuron case in Section 2.1. Consider the augmented loss $\mathcal{L}(\theta, \mathbf{w})$ in (2). Because the off-springs of the neuron are exchangeable, we can equivalently represent $\mathcal{L}(\theta, \mathbf{w})$ as a functional of the empirical measure of the off-springs,

$$\mathcal{L}[\rho] = \mathbb{E}_{x \sim \mathcal{D}} [\Phi(\mathbb{E}_{\theta \sim \rho}[\sigma(\theta, x)])], \quad \rho = \sum_{i=1}^m w_i \delta_{\theta_i}, \quad (8)$$

where δ_{θ_i} denotes the delta measure on θ_i and $\mathcal{L}[\rho]$ is the functional representation of $\mathcal{L}(\theta, \mathbf{w})$. The idea is to optimize $\mathcal{L}[\rho]$ in the space of probability distributions (or measures) using a functional steepest descent. To do so, a notion of distance on the space of distributions need to be decided. We consider the p -Wasserstein metric,

$$\mathbb{D}_p(\rho, \rho') = \inf_{\gamma \in \Pi(\rho, \rho')} (\mathbb{E}_{(\theta, \theta') \sim \gamma} [\|\theta - \theta'\|^p])^{1/p}, \quad \text{for } p > 0, \quad (9)$$

where $\Pi(\rho, \rho')$ denotes the set of probability measures whose first and second marginals are ρ and ρ' , respectively, and γ can be viewed as describing a transport plan from ρ to ρ' . We obtain the ∞ -Wasserstein metric $\mathbb{D}_\infty(\rho, \rho')$ in the limit when $p \rightarrow +\infty$, in which case the p -norm reduces to an esssup norm, that is,

$$\mathbb{D}_\infty(\rho, \rho') = \inf_{\gamma \in \Pi(\rho, \rho')} \text{esssup}_{(\theta, \theta') \sim \gamma} [\|\theta - \theta'\|],$$

where the esssup notation denotes the smallest number c such that the set $\{(\theta, \theta') : \|\theta - \theta'\| > c\}$ has zero probability under γ . See more discussion in Villani (2008) and Appendix A.2.

The ∞ -Wasserstein metric yields a natural connection to node splitting. For each θ , the conditional distribution $\gamma(\theta' | \theta)$ represents the distribution of points θ' transported from θ , which can be viewed as the off-springs of θ in the context of node splitting. If $\mathbb{D}_\infty(\rho, \rho') \leq \epsilon$, it means that ρ' can be obtained from splitting $\theta \sim \rho$ such that all the off-springs are ϵ -close, i.e., $\|\theta' - \theta\| \leq \epsilon$. This is consistent with the augmented neighborhood introduced in Section 2.1, except that γ here can be an absolutely continuous distribution, representing a continuously infinite number of off-springs; but this

yields no practical difference because any distribution γ can be approximated arbitrarily close using a countable number of particles. Note that p -Wasserstein metrics with finite p are not suitable for our purpose because $\mathbb{D}_p(\rho, \rho') \leq \epsilon$ with $p < \infty$ does not ensure $\|\theta' - \theta\| \leq \epsilon$ for all $\theta \sim \rho$ and $\theta' \sim \rho'$.

Similar to the steepest descent on the Euclidean space, the ∞ -Wasserstein steepest descent on $\mathcal{L}[\rho]$ should iteratively find new points that maximize the decrease of loss in an ϵ -ball of the current points. Define

$$\rho^* = \arg \min_{\rho'} \{\mathcal{L}[\rho'] - \mathcal{L}[\rho] : \mathbb{D}_\infty(\rho, \rho') \leq \epsilon\}, \quad \Delta^*(\rho, \epsilon) = \mathcal{L}[\rho^*] - \mathcal{L}[\rho].$$

We are ready to show the connection of Algorithm 1 to the ∞ -Wasserstein steepest descent.

Theorem 2.5. Consider the $\mathcal{L}(\theta, \mathbf{w})$ and $\mathcal{L}[\rho]$ in (2) and (8), connected with $\rho = \sum_i w_i \delta_{\theta_i}$. Define $G_\rho(\theta) = \mathbb{E}_{x \sim \mathcal{D}} [\Phi'(f_\rho(x)) \nabla_\theta \sigma(\theta, x)]$ and $S_\rho(\theta) = \mathbb{E}_{x \sim \mathcal{D}} [\Phi'(f_\rho(x)) \nabla_{\theta\theta}^2 \sigma(\theta, x)]$ with $f_\rho(x) = \mathbb{E}_{\theta \sim \rho} [\sigma(\theta, x)]$, which are related to the gradient and splitting matrices of $\mathcal{L}(\theta, \mathbf{w})$, respectively. Assume $\mathcal{L}(\theta, \mathbf{w})$ has bounded third order derivatives w.r.t. θ .

a) If $\mathcal{L}(\theta, \mathbf{w})$ is on a non-stationary point w.r.t. θ , then the steepest descent of $\mathcal{L}[\rho]$ is achieved by moving all the particles of ρ with gradient descent on $\mathcal{L}(\theta, \mathbf{w})$, that is,

$$\mathcal{L}[(I - \epsilon G_\rho) \# \rho] - \mathcal{L}[\rho] = \Delta^*(\rho, \epsilon) + \mathcal{O}(\epsilon^2) = -\epsilon \mathbb{E}_{\theta \sim \rho} [\|G_\rho(\theta)\|] + \mathcal{O}(\epsilon^2),$$

where $(I - \epsilon G_\rho) \# \rho$ denotes the distribution of $\theta' = \theta - \epsilon G_\rho(\theta) / \|G_\rho(\theta)\|$ when $\theta \sim \rho$.

b) If $\mathcal{L}(\theta, \mathbf{w})$ reaches a stable local optima w.r.t. θ , the steepest descent on $\mathcal{L}[\rho]$ is splitting each neuron with $\lambda_{\min}(S_\rho(\theta)) < 0$ into two copies of equal weights following their minimum eigenvectors, while keeping the remaining neurons to be unchanged. Precisely, denote by $(I \pm \epsilon v_{\min}(S_\rho(\theta))) \# \rho$ the distribution obtained in this way, we have

$$\mathcal{L}[(I \pm \epsilon v_{\min}(S_\rho(\theta))) \# \rho] - \mathcal{L}[\rho] = \Delta^*(\rho, \epsilon) + \mathcal{O}(\epsilon^3),$$

where we have $\Delta^*(\rho, \epsilon) = \epsilon^2 \mathbb{E}_{\theta \sim \rho} [\min(\lambda_{\min}(S_\rho(\theta)), 0)]/2$.

Remark There has been a line of theoretical works on analyzing gradient-based learning of neural networks via 2-Wasserstein gradient flow by considering the *mean field limit* when the number of neurons m goes to infinite ($m \rightarrow \infty$) (e.g., Mei et al., 2018; Chizat & Bach, 2018). These analysis focus on the first-order descent on the 2-Wasserstein space as a theoretical tool for understanding the behavior of gradient descent on overparameterized neural networks. Our framework is significant different, since we mainly consider the second-order descent on the ∞ -Wasserstein space, and the case of finite number of neurons m in order to derive practical algorithms.

3 Experiments

We test our method on both toy and realistic tasks, including learning interpretable neural networks, architecture search for image classification and energy-efficient keyword spotting. Due to limited space, many of the detailed settings are shown in Appendix, in which we also include additional results on distribution approximation (Appendix B.5).

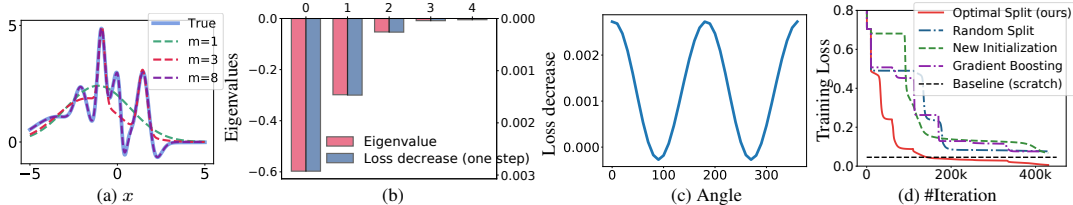


Figure 1: Results on a one-dimensional RBF network. (a) The true and estimated functions. (b) The eigenvalue vs. loss decrease. (c) The loss decrease vs. the angle of the splitting direction with the minimum eigenvector. (d) The training loss vs. the iteration (of gradient descent); the splittings happen at the cliff points.

Toy RBF Neural Networks We apply our method to learn a one-dimensional RBF neural network shown in Figure 1a. See Appendix B.1 for details of the setting. We start with a small neural network with $m = 1$ neuron and gradually increase the model size by splitting neurons. Figure 1a shows that we almost recover the true function as we split up to $m = 8$ neurons. Figure 1b shows the top five eigenvalues and the decrease of loss when we split $m = 7$ neurons to $m = 8$ neurons; we can see that the eigenvalue and loss decrease correlate linearly, confirming our results in Theorem 2.4. Figure 1c shows the decrease of the loss when we split the top one neuron following the direction with different angles from the minimum eigenvector at $m = 7$. We can see that the decrease of the loss is maximized when the splitting direction aligns with the eigenvector, consistent with our theory. In Figure 1d, we compare with different baselines of progressive training, including `Random Split`, splitting a randomly chosen neuron with a random direction; `New Initialization`, adding a new neuron with randomly initialized weights and co-optimization it with previous neurons; `Gradient Boosting`, adding new neurons with Frank-Wolfe algorithm while fixing the previous neurons; `Baseline (scratch)`, training a network of size $m = 8$ from scratch. Figure 1d shows our method yields the best result.

Learning Interpretable Neural Networks To visualize the dynamics of the splitting process, we apply our method to incrementally train an interpretable neural network designed by Li et al. (2018), which contains a “prototype layer” whose weights are enforced to be similar to realistic images to encourage interpretability. See Appendix B.2 and Li et al. (2018) for more detailed settings. We apply our method to split the prototype layer starting from a single neuron on MNIST, and show in Figure 2 the evolutionary tree of the neurons in our splitting process. We can see that the blurry (and hence less interpretable) prototypes tend to be selected and split into two off-springs that are similar yet more interpretable. Figure 2 (b) shows the decrease of loss when we split each of the five neurons at the 5-th step (with the decrease of loss measured at the local optima reached dafter splitting); we find that the eigenvalue correlates well with the decrease of loss and the interpretability of the neurons. The complete evolutionary tree and quantitative comparison with baselines are shown in Appendix B.2.

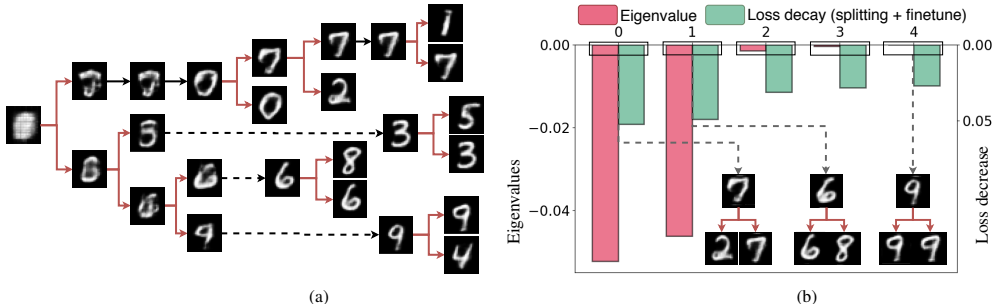


Figure 2: Progressive learning of the interpretable prototype network in Li et al. (2018) on MNIST. (a) The evolutionary tree of our splitting process, in which the least interpretable, or most ambiguous prototypes tend to be split first. (b) The eigenvalue and resulting loss decay when splitting the different neurons at the 5-th step.

Lightweight Neural Architectures for Image Classification We investigate the effectiveness of our methods in learning small and efficient network structures for image classification. We experiment with two popular deep neural architectures, MobileNet (Howard et al., 2017) and VGG19 (Simonyan & Zisserman, 2015). In both cases, we start with a relatively small network and gradually grow the network by splitting the convolution filters following Algorithm 1. See Appendix B.3 for more details of the setting. Because there is no other off-the-shelf progressive growing algorithm that can adaptively decide the neural architectures like our method, we compare with pruning methods, which follow the opposite direction of gradually removing neurons starting from a large pre-trained network. We test two state-of-the-art pruning methods, including batch-normalization-based pruning (Bn-prune) (Liu et al., 2017) and L1-based pruning (L1-prune) (Li et al., 2017). As shown in Figure 3a-b, our splitting method yields higher accuracy with similar model sizes. This is surprising and significant, because the pruning methods leverage the knowledge from a large pre-train model, while our method does not.

To further test the effect of architecture learning in both splitting and pruning methods, we test another setting in which we discard the weights of the neurons and retain the whole network starting from a random initialization, under the structure obtained from splitting or pruning at each iteration.

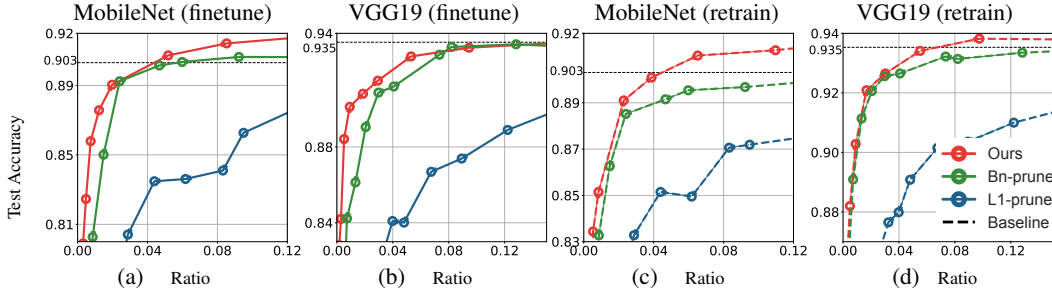


Figure 3: Results on CIFAR-10. (a)-(b) Results of Algorithm 1 and pruning methods (which successively finetune the neurons after pruning). (c)-(d) Results of Algorithm 1 and pruning methods with retraining, in which we retrain all the weights starting from random initialization after each splitting or pruning step. The x-axis represents the ratio between the number parameters of the learned models and a full size baseline network.

As shown in Figure 3c-d, the results of retraining is comparable with (or better than) the result of successive finetuning in Figure 3a-b, which is consistent with the findings in Liu et al. (2019b). Meanwhile, our splitting method still outperforms both Bn-prune and L1-prune.

Resource-Efficient Keyword Spotting on Edge Devices Keyword spotting systems aim to detect a particular keyword from a continuous stream of audio. It is typically deployed on energy-constrained edge devices and requires real-time response and high accuracy for good user experience. This casts a key challenge of constructing efficient and lightweight neural architectures. We apply our method to solve this problem, by splitting a small model (a compact version of DS-CNN) obtained from Zhang et al. (2017). See Appendix B.4 for detailed settings.

Table 1 shows the results on the Google speech commands benchmark dataset (Warden, 2018), in which our method achieves significantly higher accuracy than the best model (DS-CNN) found by Zhang et al. (2017), while having 31% less parameters and Flops. Figure 4 shows further comparison with Bn-prune (Liu et al., 2017), which is again inferior to our method.

Method	Acc	Params (K)	Ops (M)
DNN	86.94	495.7	1.0
CNN	92.64	476.7	25.3
BasicLSTM	93.62	492.6	47.9
LSTM	94.11	495.8	48.4
GRU	94.72	498.0	48.4
CRNN	94.21	485.0	19.3
DS-CNN	94.85	413.7	56.9
Ours	95.36	282.6	39.2

Table 1: Results on keyword spotting. All results are averaged over 5 rounds.

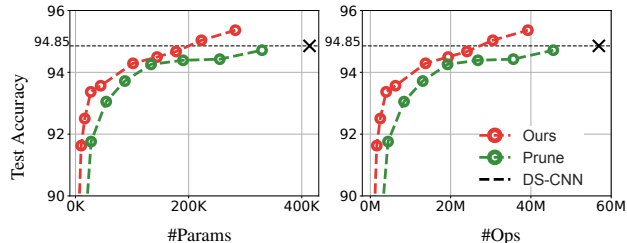


Figure 4: Comparison of accuracy vs. model size (#Params) and number of flops (#Ops) on keyword spotting.

4 Conclusion

We present a simple approach for progressively training neural networks via neuron splitting. Our approach highlights a novel view of neural structure optimization as continuous functional optimization, and yields a practical procedure with broad applications. For future work, we will further investigate fast gradient descent based approximation of large scale eigen-computation and more theoretical analysis, extensions and applications of our approach.

Acknowledgement

This work is supported in part by NSF CRII 1830161 and NSF CAREER 1846421. We would like to acknowledge Google Cloud and Amazon Web Services (AWS) for their support.

References

- Bach, Francis. Breaking the curse of dimensionality with convex neural networks. *Journal of Machine Learning Research*, 18(19):1–53, 2017.
- Bach, Francis, Lacoste-Julien, Simon, and Obozinski, Guillaume. On the equivalence between herding and conditional gradient algorithms. In *Proceedings of the 29th International Conference on Machine Learning*, pp. 1355–1362. Omnipress, 2012.
- Bengio, Yoshua, Roux, Nicolas L, Vincent, Pascal, Delalleau, Olivier, and Marcotte, Patrice. Convex neural networks. In *Advances in neural information processing systems*, pp. 123–130, 2006.
- Cai, Han, Zhu, Ligeng, and Han, Song. Proxylessnas: Direct neural architecture search on target task and hardware. In *International Conference on Learning Representation*, 2018.
- Chen, Tianqi, Goodfellow, Ian, and Shlens, Jonathon. Net2net: Accelerating learning via knowledge transfer. In *International Conference on Learning Representations*, 2016.
- Chen, Yutian, Welling, Max, and Smola, Alex. Super-samples from kernel herding. In *Conference on Uncertainty in Artificial Intelligence (UAI)*, 2010.
- Chizat, Lenaic and Bach, Francis. On the global convergence of gradient descent for over-parameterized models using optimal transport. In *Advances in neural information processing systems*, pp. 3036–3046, 2018.
- Gretton, Arthur, Borgwardt, Karsten M, Rasch, Malte J, Schölkopf, Bernhard, and Smola, Alexander. A kernel two-sample test. *Journal of Machine Learning Research*, 13(Mar):723–773, 2012.
- Han, Song, Mao, Huizi, and Dally, William J. Deep compression: Compressing deep neural networks with pruning, trained quantization and Huffman coding. *International Conference on Learning Representations*, 2016.
- Howard, Andrew G, Zhu, Menglong, Chen, Bo, Kalenichenko, Dmitry, Wang, Weijun, Weyand, Tobias, Andreetto, Marco, and Adam, Hartwig. Mobilenets: Efficient convolutional neural networks for mobile vision applications. *arXiv preprint arXiv:1704.04861*, 2017.
- Jin, Chi, Ge, Rong, Netrapalli, Praneeth, Kakade, Sham M, and Jordan, Michael I. How to escape saddle points efficiently. In *Proceedings of the 34th International Conference on Machine Learning - Volume 70*, pp. 1724–1732. JMLR. org, 2017.
- Lee, Jason D, Simchowitz, Max, Jordan, Michael I, and Recht, Benjamin. Gradient descent only converges to minimizers. In *Conference on learning theory*, pp. 1246–1257, 2016.
- Li, Hao, Kadav, Asim, Durdanovic, Igor, Samet, Hanan, and Graf, Hans Peter. Pruning filters for efficient convnets. *International Conference on Learning Representations*, 2017.
- Li, Oscar, Liu, Hao, Chen, Chaofan, and Rudin, Cynthia. Deep learning for case-based reasoning through prototypes: A neural network that explains its predictions. In *Thirty-Second AAAI Conference on Artificial Intelligence*, 2018.
- Liu, Hanxiao, Simonyan, Karen, and Yang, Yiming. Darts: Differentiable architecture search. *International Conference on Learning Representations*, 2019a.
- Liu, Zhuang, Li, Jianguo, Shen, Zhiqiang, Huang, Gao, Yan, Shoumeng, and Zhang, Changshui. Learning efficient convolutional networks through network slimming. In *Proceedings of the IEEE International Conference on Computer Vision*, pp. 2736–2744, 2017.
- Liu, Zhuang, Sun, Mingjie, Zhou, Tinghui, Huang, Gao, and Darrell, Trevor. Rethinking the value of network pruning. *International Conference on Learning Representations*, 2019b.
- Mei, Song, Montanari, Andrea, and Nguyen, Phan-Minh. A mean field view of the landscape of two-layers neural networks. *Proceedings of the National Academy of Sciences of USA*, 2018.
- Pham, Hieu, Guan, Melody, Zoph, Barret, Le, Quoc, and Dean, Jeff. Efficient neural architecture search via parameter sharing. In *International Conference on Machine Learning*, pp. 4092–4101, 2018.
- Rahimi, Ali and Recht, Benjamin. Random features for large-scale kernel machines. In *Advances in Neural Information Processing Systems*, pp. 1177–1184, 2007.
- Real, Esteban, Aggarwal, Alok, Huang, Yanping, and Le, Quoc V. Regularized evolution for image classifier architecture search. *ICML AutoML Workshop*, 2018.

- Schwenk, Holger and Bengio, Yoshua. Boosting neural networks. *Neural computation*, 12(8): 1869–1887, 2000.
- Simonyan, Karen and Zisserman, Andrew. Very deep convolutional networks for large-scale image recognition. *International Conference on Learning Representations*, 2015.
- Stanley, Kenneth O and Miikkulainen, Risto. Evolving neural networks through augmenting topologies. *Evolutionary computation*, 10(2):99–127, 2002.
- Villani, Cédric. *Optimal transport: old and new*, volume 338. Springer Science & Business Media, 2008.
- Warden, Pete. Speech commands: A dataset for limited-vocabulary speech recognition. *arXiv preprint arXiv:1804.03209*, 2018.
- Wynne-Jones, Mike. Node splitting: A constructive algorithm for feed-forward neural networks. In *Advances in neural information processing systems*, pp. 1072–1079, 1992.
- Xie, Sirui, Zheng, Hehui, Liu, Chunxiao, and Lin, Liang. SNAS: stochastic neural architecture search. *International Conference on Learning Representations*, 2018.
- Zhang, Yundong, Suda, Naveen, Lai, Liangzhen, and Chandra, Vikas. Hello edge: Keyword spotting on microcontrollers. *arXiv preprint arXiv:1711.07128*, 2017.
- Zoph, Barret and Le, Quoc V. Neural architecture search with reinforcement learning. *International Conference on Learning Representations*, 2017.

A Proofs

A.1 Proofs of Splitting Taylor Expansion

Proof of Theorem 2.2. Taking the gradient of $L(\theta)$ in (1) gives

$$\nabla_{\theta} L(\theta) = \mathbb{E}[\Phi'(\sigma(\theta, x)) \nabla_{\theta} \sigma(\theta, x)],$$

$$\nabla_{\theta\theta}^2 L(\theta) = \mathbb{E}[\Phi'(\sigma(\theta, x)) \nabla_{\theta\theta}^2 \sigma(\theta, x) + \Phi''(\sigma(\theta, x)) \nabla_{\theta} \sigma(\theta, x)^{\otimes 2}],$$

where $\Phi'(\cdot)$ is the derivative of $\Phi(\cdot)$ (which is a univariate function), and $\nabla_{\theta} \sigma(\theta, x)^{\otimes 2} := \nabla_{\theta} \sigma(\theta, x) \nabla_{\theta} \sigma(\theta, x)^{\top}$.

When θ is split into $\{w_i, \theta_i\}_{i=1}^m$, the augmented loss function is

$$\mathcal{L}(\boldsymbol{\theta}, \mathbf{w}) = \mathbb{E} \left[\Phi \left(\sum_{i=1}^m w_i \sigma(\theta_i, x) \right) \right],$$

where $\mathbf{w} = [w_1, \dots, w_m]$ and $\boldsymbol{\theta} = [\theta_1, \dots, \theta_m]$. The weights should satisfy $\sum_{i=1}^m w_i = 1$ and $w_i \geq 0$. In this way, we have $\mathcal{L}(\boldsymbol{\theta}, \mathbf{w}) = L(\theta)$ when $\boldsymbol{\theta} = [\theta, \dots, \theta] = \theta \mathbf{1}_m$.

Taking the gradient of $\mathcal{L}(\boldsymbol{\theta}, \mathbf{w})$ w.r.t. θ_i when $\boldsymbol{\theta} = \theta \mathbf{1}_m$, we have

$$\nabla_{\theta_i} \mathcal{L}(\theta \mathbf{1}_m, \mathbf{w}) = \mathbb{E}[\Phi'(\sigma(\theta, x)) w_i \nabla_{\theta} \sigma(\theta, x)] = w_i \nabla_{\theta} L(\theta).$$

Taking the second derivative, we get

$$\begin{aligned} \nabla_{\theta_i, \theta_j} \mathcal{L}(\theta \mathbf{1}_m, \mathbf{w}) &= \mathbb{E}[\Phi'(\sigma(\theta, x)) w_i \nabla_{\theta, \theta}^2 \sigma(\theta, x) + \Phi''(\sigma(\theta, x)) w_i^2 \nabla_{\theta} \sigma(\theta, x)^{\otimes 2}] \\ &:= w_i A(\theta) + w_i^2 B(\theta), \end{aligned}$$

where

$$A(\theta) := \mathbb{E}[\Phi'(\sigma(\theta, x)) \nabla_{\theta, \theta}^2 \sigma(\theta, x)], \quad B(\theta) := \mathbb{E}[\Phi''(\sigma(\theta, x)) \nabla_{\theta} \sigma(\theta, x)^{\otimes 2}].$$

Note that we have $\nabla_{\theta\theta}^2 L(\theta) = A(\theta) + B(\theta)$ following this definition.

For $i \neq j$, we have

$$\nabla_{\theta_i \theta_j} \mathcal{L}(\theta \mathbf{1}_m, \mathbf{w}) = \mathbb{E}[\Phi''(\sigma(\theta, x)) w_i w_j \nabla_{\theta} \sigma(\theta, x)^{\otimes 2}] = w_i w_j B(\theta).$$

For $\boldsymbol{\theta} = [\theta_1, \dots, \theta_m]$, assume $\theta_i = \theta + \epsilon \delta_i$, and define $\bar{\delta} = \sum_{i=1}^m w_i \delta_i$ to be the average displacement. Therefore, $\boldsymbol{\theta} = \theta \mathbf{1}_m + \epsilon \bar{\delta}$. Using the Taylor expansion of $\mathcal{L}(\theta \mathbf{1}_m + \epsilon \bar{\delta}, \mathbf{w})$ w.r.t. ϵ at $\epsilon = 0$, we have

$$\begin{aligned} \mathcal{L}(\boldsymbol{\theta}, \mathbf{w}) - L(\theta) &= \mathcal{L}(\theta \mathbf{1}_m + \epsilon \bar{\delta}, \mathbf{w}) - L(\theta) \\ &= \epsilon \sum_{i=1}^m \nabla_{\theta_i} \mathcal{L}(\theta \mathbf{1}_m, \mathbf{w})^{\top} \delta_i + \frac{\epsilon^2}{2} \sum_{ij=1}^m \delta_i^{\top} (\nabla_{\theta_i, \theta_j}^2 \mathcal{L}(\theta \mathbf{1}_m, \mathbf{w})) \delta_j + \mathcal{O}(\epsilon^3) \\ &= \epsilon \sum_{i=1}^m w_i \nabla L(\theta)^{\top} \delta_i + \frac{\epsilon^2}{2} \sum_{i=1}^m w_i \delta_i^{\top} A(\theta) \delta_i + \frac{\epsilon^2}{2} \sum_{ij=1}^m w_i w_j \delta_i^{\top} B(\theta) \delta_j + \mathcal{O}(\epsilon^3) \\ &= \epsilon \nabla L(\theta)^{\top} \bar{\delta} + \frac{\epsilon^2}{2} \sum_{i=1}^m w_i \delta_i^{\top} A(\theta) \delta_i + \frac{\epsilon^2}{2} \bar{\delta}^{\top} B(\theta) \bar{\delta} + \mathcal{O}(\epsilon^3) \\ &= \epsilon \nabla L(\theta)^{\top} \bar{\delta} + \frac{\epsilon^2}{2} \bar{\delta}^{\top} (A(\theta) + B(\theta)) \bar{\delta} + \frac{\epsilon^2}{2} \sum_{i=1}^m (\delta_i^{\top} A \delta_i - \bar{\delta}^{\top} A \bar{\delta}) + \mathcal{O}(\epsilon^3) \\ &= \epsilon \nabla L(\theta)^{\top} \bar{\delta} + \frac{\epsilon^2}{2} \bar{\delta}^{\top} \nabla^2 L(\theta) \bar{\delta} + \frac{\epsilon^2}{2} \sum_{i=1}^m (\delta_i - \bar{\delta})^{\top} A(\theta) (\delta_i - \bar{\delta}) + \mathcal{O}(\epsilon^3). \end{aligned}$$

This completes the proof. \square

Proof of Theorem 2.3. Recall that

$$H(\boldsymbol{\delta}, \mathbf{w}; \theta) = \frac{\epsilon^2}{2} \sum_{i=1}^m w_i \delta_i^{\top} S(\theta) \delta_i,$$

with $\sum_i w_i = 1$, $w_i \geq 0$ and $\|\delta_i\| = 1$. Since $\delta_i^\top S(\theta)\delta_i \geq \lambda_{\min}(S(\theta)) \|\delta_i\|^2 = \lambda_{\min}(S(\theta))$, it is obvious that

$$H(\boldsymbol{\delta}, \mathbf{w}; \theta) = \frac{\epsilon^2}{2} \sum_{i=1}^m w_i \delta_i^\top S(\theta)\delta_i \geq \frac{\epsilon^2}{2} \sum_{i=1}^m w_i \lambda_{\min}(S(\theta)) = \frac{\epsilon^2}{2} \lambda_{\min}(S(\theta)).$$

On the other hand, this lower bound is achieved by setting $m = 2$, $w_1 = w_2 = 1/2$ and $\delta_1 = -\delta_2 = v_{\min}(S(\theta))$. This completes the proof. \square

Proof of Theorem 2.4. Step 1: We first consider the case with no average displacement, that is, $\mu^{[\ell]} = 0$. In this case, Lemma A.1 below gives

$$\mathcal{L}(\boldsymbol{\theta}^{[1:n]}, \mathbf{w}^{[1:n]}) = L(\theta^{[1:n]}) + \sum_{\ell=1}^n \left(\mathcal{L}(\boldsymbol{\theta}_\ell^{[1:n]}, \mathbf{w}^{[1:n]}) - L(\theta^{[1:n]}) \right) + \mathcal{O}(\epsilon^3), \quad (10)$$

where $\boldsymbol{\theta}_\ell^{[1:n]}$ denotes the augmented parameters obtained when we only split the ℓ -th neuron, while keeping all the neurons unchanged. Applying Theorem 2.2, we have for each ℓ ,

$$\mathcal{L}(\boldsymbol{\theta}_\ell^{[1:n]}, \mathbf{w}^{[1:n]}) - L(\theta^{[1:n]}) = \frac{\epsilon^2}{2} H_\ell(\boldsymbol{\delta}^{[\ell]}, \mathbf{w}^{[\ell]}; \theta^{[1:n]}) + \mathcal{O}(\epsilon^3).$$

Combining this with (10) yields the result.

Step 2: We now consider the more general case when $\mu^{[1:n]} \neq 0$. Let $\tilde{\theta}^{[1:n]} = \theta^{[1:n]} + \epsilon\mu^{[1:n]}$. Applying the result above on $\tilde{\theta}^{[1:n]}$, we have

$$\mathcal{L}(\boldsymbol{\theta}^{[1:n]}, \mathbf{w}^{[1:n]}) = L(\tilde{\theta}^{[1:n]}) + \frac{\epsilon^2}{2} D(\tilde{\theta}^{[1:n]}) + \mathcal{O}(\epsilon^3)$$

where $D(\tilde{\theta}^{[1:n]}) := \sum_{\ell=1}^n H_\ell(\boldsymbol{\delta}^{[\ell]}, \mathbf{w}^{[\ell]}; \tilde{\theta}^{[1:n]})$. Therefore,

$$\begin{aligned} \mathcal{L}(\boldsymbol{\theta}^{[1:n]}, \mathbf{w}^{[1:n]}) &= L(\tilde{\theta}^{[1:n]}) + \frac{\epsilon^2}{2} D(\tilde{\theta}^{[1:n]}) + \mathcal{O}(\epsilon^3) \\ &= L(\tilde{\theta}^{[1:n]}) + \frac{\epsilon^2}{2} D(\theta^{[1:n]}) + \frac{\epsilon^2}{2} (D(\tilde{\theta}^{[1:n]}) - D(\theta^{[1:n]})) + \mathcal{O}(\epsilon^3) \\ &= L(\tilde{\theta}^{[1:n]}) + \frac{\epsilon^2}{2} D(\theta^{[1:n]}) + \mathcal{O}(\epsilon^3) \quad // \text{because } \theta^{[1:n]} - \tilde{\theta}^{[1:n]} = \mathcal{O}(\epsilon) \\ &= L(\theta^{[1:n]} + \epsilon\mu^{[1:n]}) + \frac{\epsilon^2}{2} D(\theta^{[1:n]}) + \mathcal{O}(\epsilon^3), \end{aligned}$$

where $D(\theta^{[1:n]}) := \sum_{\ell=1}^n H_\ell(\boldsymbol{\delta}^{[\ell]}, \mathbf{w}^{[\ell]}; \theta^{[1:n]})$. This completes the proof. \square

Lemma A.1. Let $\theta^{[1:n]}$ be the parameters of n neurons. Recall that we assume $\theta^{[\ell]}$ is split into m_ℓ off-springs with parameters $\boldsymbol{\theta}^{[\ell]} = \{\theta_i^{[\ell]}\}_{i=1}^{m_\ell}$ and weights $\mathbf{w}^{[\ell]} = \{w_i^{[\ell]}\}_{i=1}^{m_\ell}$, which satisfies $\sum_{i=1}^{m_\ell} w_i^{[\ell]} = 1$. Let $\theta_i^{[\ell]} = \theta^{[\ell]} + \epsilon\delta_i^{[\ell]}$, where $\delta_i^{[\ell]}$ is the perturbation on the i -th off-spring of the ℓ -th neuron. Assume $\bar{\delta}^{[\ell]} := \sum_{i=1}^{m_\ell} w_i^{[\ell]} \delta_i^{[\ell]} = 0$, that is, the average displacement of all the neurons is zero.

Denote by $\boldsymbol{\theta}_\ell^{[1:n]}$ the augmented parameters we obtained by only splitting the ℓ -th neuron while keeping all the other neurons unchanged, that is, we have $\theta_{\ell,i}^{[\ell]} = \theta^{[\ell]} + \epsilon\delta_i^{[\ell]}$ for $i = 1, \dots, m_\ell$, and $\theta_{\ell,i}^{[\ell']} = \theta^{[\ell']}$ for all $\ell' \neq \ell$ and $i = 1, \dots, m_{\ell'}$. Assume the third order derivatives of $\mathcal{L}(\boldsymbol{\theta}^{[1:n]}, \mathbf{w}^{[1:n]})$ are bounded. We have

$$\mathcal{L}(\boldsymbol{\theta}^{[1:n]}, \mathbf{w}^{[1:n]}) = L(\theta^{[1:n]}) + \sum_{\ell=1}^n \left(\mathcal{L}(\boldsymbol{\theta}_\ell^{[1:n]}, \mathbf{w}^{[1:n]}) - L(\theta^{[1:n]}) \right) + \mathcal{O}(\epsilon^3).$$

Proof. Define

$$F := \left(\mathcal{L}(\boldsymbol{\theta}^{[1:n]}, \mathbf{w}^{[1:n]}) - L(\boldsymbol{\theta}^{[1:n]}) \right) - \sum_{\ell=1}^n \left(\mathcal{L}(\boldsymbol{\theta}_\ell^{[1:n]}, \mathbf{w}^{[1:n]}) - L(\boldsymbol{\theta}^{[1:n]}) \right).$$

By Taylor expansion,

$$F = \epsilon \nabla_\epsilon F|_{\epsilon=0} + \frac{\epsilon^2}{2} \nabla_{\epsilon\epsilon} F|_{\epsilon=0} + \mathcal{O}(\epsilon^3).$$

It is obvious to see that the first order derivation $\nabla_\epsilon F|_{\epsilon=0}$ equals zero because of the correction terms. Specifically,

$$\nabla_\epsilon F|_{\epsilon=0} = \sum_{\ell=1}^n \sum_{i=1}^{m_\ell} \nabla_{\theta_i^{[\ell]}} \mathcal{L}(\boldsymbol{\theta}^{[1:n]}, \mathbf{w}^{[1:n]})^\top \delta_i^{[\ell]} \Big|_{\epsilon=0} - \sum_{\ell=1}^n \sum_{i=1}^{m_\ell} \nabla_{\theta_i^{[\ell]}} \mathcal{L}(\boldsymbol{\theta}^{[1:n]}, \mathbf{w}^{[1:n]})^\top \delta_i^{[\ell]} \Big|_{\epsilon=0} = 0.$$

For the second order derivation, define

$$A_{\ell, \ell'} = \nabla_{\theta^{[\ell]} \theta^{[\ell']}} L(\boldsymbol{\theta}^{[1:n]}).$$

For any $\ell \neq \ell'$, we have from (5) and (6) that

$$\nabla_{\theta_i^{[\ell]} \theta_{i'}^{[\ell']}} \mathcal{L}(\boldsymbol{\theta}^{[1:n]}, \mathbf{w}^{[1:n]}) \Big|_{\epsilon=0} = w_i^{[\ell]} w_{i'}^{[\ell']} \nabla_{\theta^{[\ell]} \theta^{[\ell']}} L(\boldsymbol{\theta}^{[1:n]}) = w_i^{[\ell]} w_{i'}^{[\ell']} A_{\ell, \ell'}.$$

Therefore, we have

$$\begin{aligned} \nabla_{\epsilon\epsilon} F|_{\epsilon=0} &= \sum_{\ell \neq \ell'} \sum_{i=1}^{m_\ell} \sum_{i'=1}^{m_{\ell'}} (\delta_i^{[\ell]})^\top \nabla_{\theta_i^{[\ell]} \theta_{i'}^{[\ell']}} \mathcal{L}(\boldsymbol{\theta}^{[1:n]}, \mathbf{w}^{[1:n]}) \Big|_{\epsilon=0} \delta_{i'}^{[\ell']} \\ &= \sum_{\ell \neq \ell'} \sum_{i=1}^{m_\ell} \sum_{i'=1}^{m_{\ell'}} w_i^{[\ell]} w_{i'}^{[\ell']} (\delta_i^{[\ell]})^\top A_{\ell, \ell'} \delta_{i'}^{[\ell']} \\ &= \sum_{\ell \neq \ell'} (\bar{\delta}^{[\ell]})^\top A_{\ell, \ell'} \bar{\delta}^{[\ell']} \\ &= 0 \quad // \text{because } \bar{\delta}^{[\ell]} = 0, \end{aligned}$$

where $\nabla_{\epsilon\epsilon} F|_{\epsilon=0}$ only involves cross derivatives $\nabla_{\theta_i^{[\ell]} \theta_{i'}^{[\ell']}} \mathcal{L}(\boldsymbol{\theta}^{[1:n]}, \mathbf{w}^{[1:n]})$ with $\ell \neq \ell'$, because all the terms with $\ell = \ell'$ are cancelled due to the correction terms. \square

A.2 Proofs of ∞ -Wasserstein Steepest Descent

Recall that p -Wasserstein distance is

$$W_p(\rho, \rho') = \inf_{\gamma \in \Pi(\rho, \rho')} \mathbb{E}_{(\theta, \theta') \sim \gamma} [\|\theta - \theta'\|^p]^{1/p}.$$

When $p \rightarrow +\infty$, we obtain ∞ -Wasserstein distance,

$$W_\infty(\rho, \rho') = \inf_{\gamma \in \Pi(\rho, \rho')} \text{esssup}_{(\theta, \theta') \sim \gamma} \|\theta - \theta'\|, \quad (11)$$

where esssup denotes essential supremum; it is the minimum value c with $\gamma(\|\theta - \theta'\| \geq c) = 0$.

In the proof, we denote by $\gamma_{\rho, \rho'}$ an optimal solution of γ in (11), that is,

$$\gamma_{\rho, \rho'} \in \arg \inf_{\gamma \in \Pi(\rho, \rho')} \text{esssup}_{(\theta, \theta') \sim \gamma} \|\theta - \theta'\|.$$

$\gamma_{\rho, \rho'}$ is called an ∞ -Wasserstein optimal coupling of ρ and ρ' . Denote by $\mu_{\rho, \rho'}(\theta)$ and $\Sigma_{\rho, \rho'}(\theta)$ the mean and covariance matrix of $(\theta' - \theta)$ under $\gamma_{\rho, \rho'}$, conditional on θ , that is,

$$\mu_{\rho, \rho'}(\theta) = \mathbb{E}_{\gamma_{\rho, \rho'}}[(\theta' - \theta) \mid \theta] \quad \Sigma_{\rho, \rho'}(\theta) = \text{cov}_{\gamma_{\rho, \rho'}}[(\theta' - \theta) \mid \theta].$$

It is natural to expect that we can upper bound the magnitude of both $\mu_{\rho, \rho'}(\theta)$ and $\Sigma_{\rho, \rho'}(\theta)$ by the ∞ -Wasserstein distance.

Lemma A.2. *Following the definition above, we have*

$$\|\mu_{\rho, \rho'}(\theta)\| \leq W_\infty(\rho, \rho'), \quad \lambda_{max}(\Sigma_{\rho, \rho'}(\theta)) \leq W_\infty(\rho, \rho')^2,$$

almost surely for $\theta \sim \rho$.

Proof. We have

$$\|\mu_{\rho, \rho'}(\theta)\| \leq \operatorname{esssup}_{\gamma_{\rho, \rho'}} \|\theta - \theta'\| = W_\infty(\rho, \rho'),$$

almost surely for $\theta \sim \rho$. And

$$\begin{aligned} \lambda_{max}(\Sigma_{\rho, \rho'}(\theta)) &= \max_{\|v\|=1} \operatorname{var}_{\gamma_{\rho, \rho'}} [v^\top (\theta' - \theta) \mid \theta] \\ &\leq \max_{\|v\|=1} \mathbb{E}_{\gamma_{\rho, \rho'}} \left[(v^\top (\theta' - \theta))^2 \mid \theta \right] \\ &\leq \operatorname{esssup}_{\gamma_{\rho, \rho'}} \|\theta - \theta'\|^2 \\ &= W_\infty(\rho, \rho')^2. \end{aligned}$$

□

Theorem A.3. *Define $G_\rho(\theta) = \mathbb{E}_{x \sim \mathcal{D}} [\nabla \Phi(\mathbb{E}_\rho[\sigma(\theta, x)]) \nabla \sigma(\theta, x)]$. For two distributions ρ and ρ' and their ∞ -Wasserstein optimal coupling $\gamma_{\rho, \rho'}$. We have*

$$\mathcal{L}[\rho'] = \mathcal{L}[\rho] + \mathbb{E}_{\theta \sim \rho} [G_\rho(\theta)^\top \mu_{\rho, \rho'}(\theta)] + \mathcal{O}((\mathbb{D}_\infty(\rho, \rho'))^2). \quad (12)$$

Proof. We write $\gamma = \gamma_{\rho, \rho'}$ for convenience. Denote by $\nabla \sigma(\theta, x) = \nabla_\theta \sigma(\theta, x)$ and $\nabla^2 \sigma(\theta, x) = \nabla_{\theta\theta}^2 \sigma(\theta, x)$ the first and second order derivatives of σ in terms of its first variable.

For $(\theta, \theta') \sim \gamma$, introduce $\theta_\eta = \eta\theta' + (1-\eta)\theta$, whose distribution is denoted by ρ_η . We have $\rho_0 = \rho$ and $\rho_1 = \rho'$. Taking Taylor expansion of $\mathcal{L}[\rho_\eta]$ w.r.t. η , we have

$$\mathcal{L}[\rho'] = \mathcal{L}[\rho] + \nabla_\eta \mathcal{L}[\rho_\eta] \Big|_{\eta=0} + \frac{1}{2} \nabla_{\eta\eta}^2 \mathcal{L}[\rho_\eta] \Big|_{\eta=\xi},$$

where ξ is a number between 0 and 1. We just need to calculate the derivatives. For the first order derivative, we have

$$\begin{aligned} \nabla_\eta \mathcal{L}[\rho_\eta] \Big|_{\eta=0} &= \nabla_\eta \mathbb{E}_{x \sim \mathcal{D}} [\Phi(\mathbb{E}_\gamma[\sigma(\eta\theta' + (1-\eta)\theta, x)])] \Big|_{\eta=0} \\ &= \mathbb{E}_{x \sim \mathcal{D}} [\Phi'(\mathbb{E}_\gamma[\sigma(\theta_\eta, x)]) \mathbb{E}_\gamma[\nabla \sigma(\theta_\eta, x)^\top (\theta' - \theta)]] \Big|_{\eta=0} \\ &= \mathbb{E}_{x \sim \mathcal{D}} [\Phi'(\mathbb{E}_\gamma[\sigma(\theta, x)]) \mathbb{E}_\gamma[\nabla \sigma(\theta, x)^\top (\theta' - \theta)]] \\ &= \mathbb{E}_\gamma[G_\rho(\theta)^\top (\theta' - \theta)] \\ &= \mathbb{E}_\rho[G_\rho(\theta)^\top \mu_{\rho, \rho'}(\theta)], \end{aligned}$$

where we used the derivation of $G_\rho(\theta)$.

For the second order derivative, we have

$$\begin{aligned} \nabla_{\eta\eta}^2 \mathcal{L}[\rho_\eta] \Big|_{\eta=\xi} &= \nabla_\eta (\nabla_\eta \mathcal{L}[\rho_\eta]) \Big|_{\eta=\xi} \\ &= \nabla_\eta \mathbb{E}_{x \sim \mathcal{D}} [\Phi'(\mathbb{E}_\gamma[\sigma(\theta_\eta, x)]) \mathbb{E}_\gamma[\nabla \sigma(\theta_\eta, x)^\top (\theta' - \theta)]] \Big|_{\eta=\xi} \\ &= \mathbb{E}_{x \sim \mathcal{D}} [\Phi''(\mathbb{E}_\gamma[\sigma(\theta_\eta, x)]) (\mathbb{E}_\gamma[\nabla \sigma(\theta_\eta, x)^\top (\theta' - \theta)])^2] \\ &\quad + \mathbb{E}_{x \sim \mathcal{D}} [\Phi'(\mathbb{E}_\gamma[\sigma(\theta_\eta, x)]) \mathbb{E}_\gamma[(\theta' - \theta)^\top \nabla^2 \sigma(\theta_\eta, x) (\theta' - \theta)]] \Big|_{\eta=\xi} \\ &= \mathbb{E}_\gamma[(\theta' - \theta)^\top T_\rho(\theta_\xi) (\theta' - \theta)] + \mathbb{E}_\gamma[(\theta' - \theta)^\top S_\rho(\theta_\xi) (\theta' - \theta)] \\ &= \mathbb{E}_\gamma[(\theta' - \theta)^\top (T_\rho(\theta_\xi) + S_\rho(\theta_\xi)) (\theta' - \theta)] \end{aligned}$$

where we define $T_\rho(\theta_\xi) := \mathbb{E}_{x \sim \mathcal{D}} [\Phi''(\mathbb{E}_\gamma[\sigma(\theta_\xi, x)]) \nabla \sigma(\theta_\xi, x)^{\otimes 2}]$. Denote by $\lambda_* := \sup_{\xi \in [0,1]} \lambda_{\max}(T_\rho(\theta_\xi) + S_\rho(\theta_\xi))$. We have

$$\begin{aligned} \nabla_{\eta\eta}^2 \mathcal{L}[\rho_\eta] \Big|_{\eta=\xi} &\leq \lambda_* \mathbb{E}_\gamma [\|\theta' - \theta\|^2] \\ &= \mathcal{O} \left(\mathbb{E}_\gamma [\|\theta' - \theta\|^2] \right) \\ &= \mathcal{O} \left(\left[\operatorname{esssup}_\gamma \|\theta' - \theta\| \right]^2 \right) \\ &= \mathcal{O}(\mathbb{D}_\infty(\rho, \rho')^2). \end{aligned}$$

This completes the proof. \square

Theorem A.4. For two distributions ρ and ρ' , denote by $\gamma_{\rho, \rho'}$ their ∞ -Wasserstein optimal coupling, and $\mu_{\rho, \rho'}(\theta)$ and $\Sigma_{\rho, \rho'}(\theta)$ the mean and covariance matrix of $(\theta' - \theta)$ under $\gamma_{\rho, \rho'}$, conditional on θ , respectively. Denote by $(I + \mu_{\rho, \rho'}) \# \rho$ the distribution of $\theta + \mu_{\rho, \rho'}(\theta)$ when $\theta \sim \rho$. We have

$$\mathcal{L}[\rho'] = \mathcal{L}[(I + \mu_{\rho, \rho'}) \# \rho] + \mathbb{E}_{\theta \sim \rho} \left[\frac{1}{2} \operatorname{tr}(S_\rho(\theta)^\top \Sigma_{\rho, \rho'}(\theta)) \right] + \mathcal{O}((\mathbb{D}_\infty(\rho, \rho'))^3) \quad (13)$$

where $S_\rho(\theta) = \mathbb{E}_{x \sim \mathcal{D}} [\Phi'(f_\rho(x)) \nabla_{\theta\theta}^2 \sigma(\theta, x)]$. The first and second terms capture the effect of displacement and splitting, respectively.

Proof of Theorem A.4. We use $\gamma := \gamma_{\rho, \rho'}$ for notation convenience. Denote by $\tilde{\theta} = \theta + \mu_{\rho, \rho'}(\theta)$ and $\tilde{\rho} = (I + \mu_{\rho, \rho'}) \# \rho$ the distribution of $\tilde{\theta}$ when $\theta \sim \rho$. Recall that for $(\theta, \theta') \sim \gamma$, we have

$$\mathbb{E}_\gamma \left[\theta' - \tilde{\theta} \mid \theta \right] = \mathbb{E}_\gamma [\theta' - \theta - \mu_{\rho, \rho'}(\theta) \mid \theta] = 0, \quad (14)$$

$$\Sigma_{\rho, \rho'}(\theta) = \mathbb{E}_\gamma \left[(\theta' - \tilde{\theta})(\theta' - \tilde{\theta})^\top \mid \theta \right]. \quad (15)$$

Introduce $\theta_\eta = \eta\theta' + (1 - \eta)\tilde{\theta}$. Denote by ρ_η the distribution of θ_η . This gives $\rho' = \rho_1$ and $\tilde{\rho} = \rho_0$. We have

$$\mathcal{L}[\rho'] = \mathcal{L}[\tilde{\rho}] + \nabla_\eta \mathcal{L}[\rho_\eta] \Big|_{\eta=0} + \frac{1}{2} \nabla_{\eta\eta}^2 \mathcal{L}[\rho_\eta] \Big|_{\eta=0} + \frac{1}{6} \nabla_{\eta\eta\eta}^3 \mathcal{L}[\rho_\eta] \Big|_{\eta=\xi},$$

where ξ is a number between 0 and 1. We just need to evaluate these derivatives. For the first order derivative, we have

$$\begin{aligned} \nabla_\eta \mathcal{L}[\rho_\eta] \Big|_{\eta=0} &= \nabla_\eta \mathbb{E}_{x \sim \mathcal{D}} \left[\Phi \left(\mathbb{E}_\gamma [\sigma(\eta\theta' + (1 - \eta)\tilde{\theta}, x)] \right) \right] \Big|_{\eta=0} \\ &= \mathbb{E}_{x \sim \mathcal{D}} \left[\Phi' \left(\mathbb{E}_\gamma [\sigma(\theta_\eta, x)] \right) \mathbb{E}_\gamma [\nabla \sigma(\theta_\eta, x)^\top (\theta' - \tilde{\theta})] \right] \Big|_{\eta=0} \\ &= \mathbb{E}_{x \sim \mathcal{D}} \left[\Phi' \left(\mathbb{E}_\gamma [\sigma(\tilde{\theta}, x)] \right) \mathbb{E}_\gamma [\nabla \sigma(\tilde{\theta}, x)^\top (\theta' - \tilde{\theta})] \right] \\ &= 0, \end{aligned}$$

where the last step uses (14). Here $\nabla \sigma$ denote the derivatives w.r.t. its first variables.

For the second order derivative, we have

$$\begin{aligned}
& \nabla_{\eta\eta}^2 \mathcal{L}[\rho_\eta] \Big|_{\eta=0} = \nabla_\eta (\nabla_\eta \mathcal{L}[\rho_\eta]) \Big|_{\eta=0} \\
& = \nabla_\eta \mathbb{E}_{x \sim \mathcal{D}} \left[\Phi' (\mathbb{E}_\gamma [\sigma(\theta_\eta, x)]) \mathbb{E}_\gamma [\nabla \sigma(\theta_\eta, x)^\top (\theta' - \tilde{\theta})] \right] \Big|_{\eta=0} \\
& = \mathbb{E}_{x \sim \mathcal{D}} \left[\Phi'' (\mathbb{E}_\gamma [\sigma(\theta_\eta, x)]) (\mathbb{E}_\gamma [\nabla \sigma(\theta_\eta, x) (\theta' - \tilde{\theta})])^2 \right] \\
& \quad + \mathbb{E}_{x \sim \mathcal{D}} \left[\Phi' (\mathbb{E}_\gamma [\sigma(\theta_\eta, x)]) \mathbb{E}_\gamma [(\theta' - \tilde{\theta})^\top \nabla^2 \sigma(\theta_\eta, x) (\theta' - \tilde{\theta})] \right] \Big|_{\eta=0} \quad (16) \\
& = 0 + \mathbb{E}_\gamma [(\theta' - \tilde{\theta})^\top S_\rho(\theta) (\theta' - \tilde{\theta})] \\
& = \mathbb{E}_{\theta \sim \rho} [\text{tr}(S_\rho(\theta) \Sigma_{\rho, \rho'}(\theta))].
\end{aligned}$$

Further, we can show that $\nabla_{\eta\eta\eta}^3 \mathcal{L}[\rho_\eta] \Big|_{\eta=\xi} = \mathcal{O}(\mathbb{D}_\infty(\rho, \rho')^3)$, since when taking the third gradient, all the terms of the derivative are bounded by $\|\theta - \theta'\|^3$. Specifically, taking the derivative of the form of $\nabla_{\eta\eta}^2 \mathcal{L}[\rho_\eta]$ in (16) gives

$$\begin{aligned}
& \nabla_{\eta\eta\eta}^3 \mathcal{L}[\rho_\eta] \Big|_{\eta=\xi} \\
& = \mathbb{E}_{x \sim \mathcal{D}} \left[\Phi''' (\mathbb{E}_\gamma [\sigma(\theta_\xi, x)]) (\mathbb{E}_\gamma [\nabla \sigma(\theta_\xi, x) (\theta' - \tilde{\theta})])^3 \right] \\
& \quad + 3 \mathbb{E}_{x \sim \mathcal{D}} \left[\Phi'' (\mathbb{E}_\gamma [\sigma(\theta_\xi, x)]) \mathbb{E}_\gamma [\nabla \sigma(\theta_\xi, x) (\theta' - \tilde{\theta})] \mathbb{E}_\gamma [(\theta' - \tilde{\theta})^\top \nabla^2 \sigma(\theta_\xi, x) (\theta' - \tilde{\theta})] \right] \\
& \quad + \mathbb{E}_{x \sim \mathcal{D}} \left[\Phi' (\mathbb{E}_\gamma [\sigma(\theta_\xi, x)]) \mathbb{E}_\gamma [\langle \nabla^3 \sigma(\theta_\xi, x), (\theta' - \tilde{\theta})^{\otimes 3} \rangle] \right] \\
& = \mathcal{O} \left(\text{esssup}_{(\theta, \theta') \sim \rho} \|\theta' - \tilde{\theta}\|^3 \right) \\
& = \mathcal{O}(\mathbb{D}_\infty(\rho, \rho')^3).
\end{aligned}$$

Here we use the notation $\langle A, v^{\otimes 3} \rangle = \sum_{ijk=1}^d A_{ijk} v_i v_j v_k$. This completes the proof. \square

Proof of Theorem 2.5. Following Theorem A.3, we have

$$\Delta^*(\rho, \epsilon) = \min_{\rho'} \left\{ \mathbb{E}_{\theta \sim \rho} [G_\rho(\theta)^\top \mu_{\rho, \rho'}(\theta)] : \mathbb{D}_\infty(\rho, \rho') \leq \epsilon \right\} + \mathcal{O}(\epsilon^2).$$

For $\mathbb{D}_\infty(\rho, \rho') \leq \epsilon$, we must have $\|\mu_{\rho, \rho'}\| \leq \epsilon$, and hence $\mathbb{E}_{(\theta, \theta') \sim \gamma_{\rho, \rho'}} [G_\rho(\theta)^\top \mu_{\rho, \rho'}(\theta)] \geq -\epsilon \mathbb{E}_\rho [\|G_\rho(\theta)\|]$ by Cauchy–Schwarz inequality. On the other hand, this minimum is achieved when $\mu_{\rho, \rho'} = -\epsilon G_\rho(\theta) / \|G_\rho(\theta)\|$. The only distribution ρ' that satisfies this condition is $\rho' = (I - \epsilon G_\rho(\theta) / \|G_\rho(\theta)\|) \# \rho$. This proves Theorem 2.5a.

For Theorem 2.5b, we need to use the result in Theorem A.4, which yields, in the case of stable local optima, that

$$\Delta^*(\rho, \epsilon) = \min_{\rho'} \left\{ \mathbb{E}_{\theta \sim \rho} \left[\frac{1}{2} \text{tr}(S_\rho(\theta)^\top \Sigma_{\rho, \rho'}(\theta)) \right] : \mathbb{D}_\infty(\rho, \rho') \leq \epsilon \right\} + \mathcal{O}(\epsilon^3).$$

Similar to the argument above, the minima should satisfy $\Sigma_{\rho, \rho'}(\theta) \propto v_{\min} v_{\min}^\top$, where v_{\min} is the eigenvector of $S_\rho(\theta)$ associated with its minimum eigenvalue. This corresponds to splitting θ into two copies with each weights with parameter $\theta \pm \epsilon v_{\min}$ when $\lambda_{\min} < 0$, or keep ρ unchanged when $\lambda_{\min} > 0$. \square

B Experimental Settings and Additional Results

B.1 Two-Layer RBF Neural network

We consider fitting a simple radial basis function (RBF) neural network of form

$$f(x) = \sum_{i=1}^m \sigma(\theta_i, x), \quad \sigma(\theta, x) := \theta_{i,3} \times \exp\left(-\frac{1}{2}(\theta_{i,1}x + \theta_{i,2})^2\right),$$

where $x \in \mathbb{R}$ and $\theta_i = [\theta_{i,1}, \theta_{i,2}, \theta_{i,3}]^\top \in \mathbb{R}^3$. For the ground truth, we set $m = 15$ and sample the true values of parameters $\{\theta_i\}$ from $\mathcal{N}(0, 3)$, yielding the light blue curves shown in Figure 5. We generate a training data set $\mathcal{D} := \{x_i, y_i\}_{i=1}^{1000}$ by drawing x_i from $\text{Uniform}[-5, 5]$ and set $y_i = f_*(x_i)$ without noise, where f_* denotes the true network we sampled. The network is trained by minimizing the mean square loss:

$$\min_f \mathbb{E}_{x \sim \mathcal{D}} [(f_*(x) - f(x))^2].$$

Mapping to (2), we have $\Phi(f) = (f_* - f)^2$. We learn the function using our splitting method and other progressive training baselines, all starting from $m = 1$ neuron. We add one additional neuron in each splitting/growing phase for all the methods. The parametric descent phase is performed using typical stochastic gradient descent until convergence. We stop the splitting process at $m = 8$ for all the methods. Figure 5 shows curves learned by different methods with $m = 3$ and $m = 8$ neurons, respectively. Our method yields better approximation.

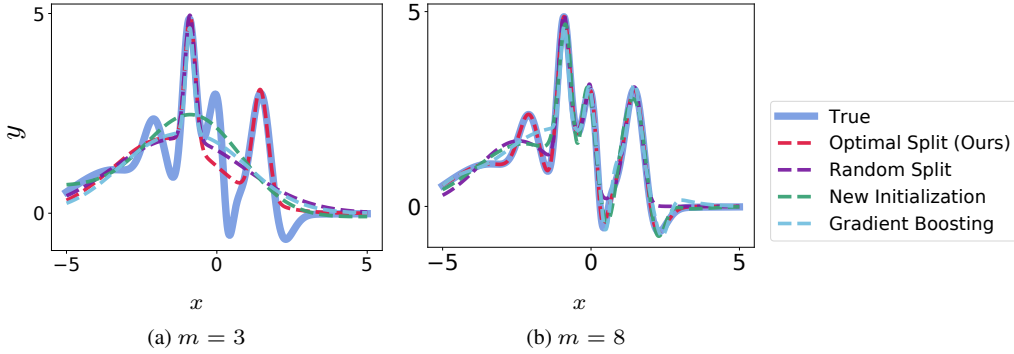


Figure 5: Results on the toy RBF neural network.

B.2 Learning Interpretable Neural Network

We provide more details on learning the interpretable neural network.

Setting We adopt the interpretable neural architecture proposed in Li et al. (2018) as our testbed. Unlike standard black-box neural networks, this architecture contains a special prototype layer in the classifier, which includes a set of prototype neurons that are enforced to encode to realistic images for promoting interpretability. In this model, each input image x is first mapped to a lower-dimensional representation based on its distance $\|\theta - e(x)\|$ with a set of prototype vectors, where $\theta \in \mathbb{R}^{40}$ represents a prototype vector and $e(x)$ is an encoder function. The prototype vectors are enforced to be interpretable in that they can be decoded to some realistic images; this is achieved in Li et al. (2018) by introducing a regularization term that minimizes the minimum square distance between the prototypes and the training data, that is, $\min_i \|\theta - e(x_i)\|$, where $\{x_i\}$ denotes the training dataset.

We apply our method to split the prototype neurons, by treating $\sigma(\theta, x) := \|\theta - e(x)\|$ as the activation function. We use the MNIST dataset in our experiment. We visualize the prototype neurons we learned using the images that they encode, by feeding the prototype vectors θ into a decoder function jointly trained with the network. We use the same encoder and decoder architectures, as suggested in Li et al. (2018) and refer the reader to Li et al. (2018) for more implementation details. To better understand the splitting dynamics, we start with a small network with just one prototype neuron and gradually add more prototypes via splitting.

We compare our method with two baseline methods, `New Initialization` and `Random Split`, that also progressively grow the prototype layers starting from one prototype neuron. In `New Initialization`, we simply add one new prototype neuron with random initialization at each iteration. In `Random Split`, we randomly pick a prototype neuron to split and split it following its splitting gradient given by our splitting matrix. Figure 6 visualizes the full splitting/growing process of our method and the two baselines. We can see that our splitting method successfully identifies the most ambiguous (and least interpretable) prototype neurons to split at each iteration, and achieves the best final results.

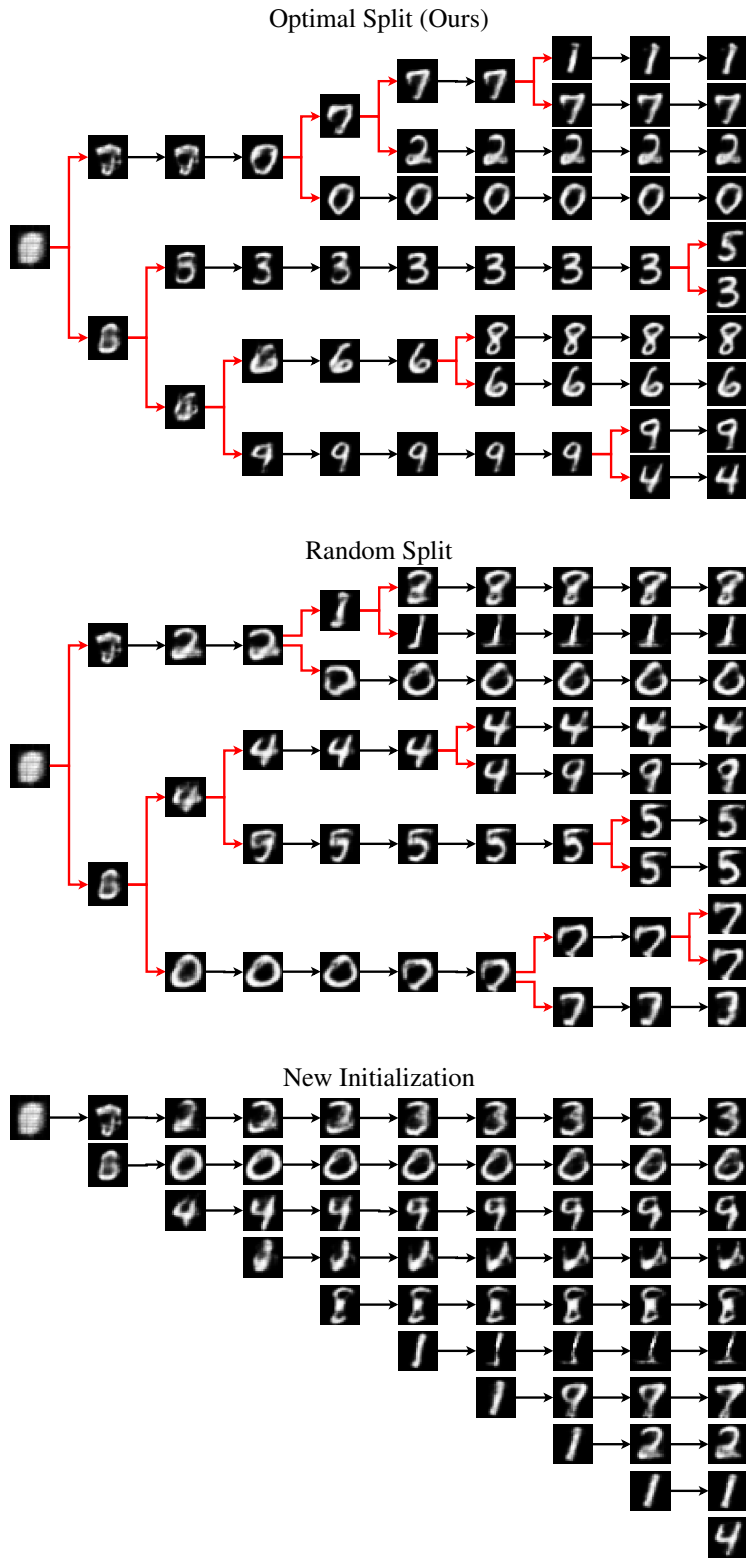


Figure 6: Visualizing the growing process of the prototype neurons given by our splitting method and the two baselines.

B.3 Lightweight Neural Architectures for Image Classification

We describe details of our experiments on learning lightweight deep networks for image classification.

Dataset and Backbone Networks We use the CIFAR-10 benchmark dataset. We adopt a standard data argumentation scheme (mirroring and shifting) that is widely used for this dataset (Liu et al., 2019b, 2017). The input images are normalized using channel means and standard derivations. We use two popular deep neural architectures as our testbed, MobileNet (Howard et al., 2017) and VGG19 (Simonyan & Zisserman, 2015).

Training Settings We treat the filters as the neurons to split for convolutional neural networks. For example, consider a convolutional layer with $n_{out} \times n_{in} \times k \times k$ parameters, where n_{out} denotes the number of output channels and n_{in} the number of input channels and k the filter size. We treat it as n_{out} neurons, and each neuron has a parameter of size $n_{in} \times k \times k$. To apply our methods, we start with a small variant of the MobileNet and VGG19, and gradually grow the network by splitting the (convolutional) neurons with the most negative splitting indexes following Algorithm 1. For MobileNet, we construct the initial network by keeping the size of the first convolution layer as the same (=32) as the original MobileNet and setting the number of depthwise and pointwise channels to be 16. For VGG19, we set the number of channels of the initial network to be 16 for all layers.

For the parametric descent phase, we use stochastic gradient descent with an initial learning rate 0.1 for 160 epochs. The learning rate is divided by 10 at 50% and 75% of the total number of training epochs. We use a weight decay of 10^{-4} and a Nesterove momentum of 0.9 without dampening. The batch size is set to be 64. In each splitting phase, we increase the number of channels by a percentage of 30 using our method.

Note that our splitting matrix (see Eq. 7) involves the second-order derivative of the activation function, which is not well defined for ReLU activation. Therefore, we replace the ReLU activation with Softplus to prevent numerical issues in calculating the splitting matrices. We also apply Softplus in the other experiments that contain ReLU activation function in the network.

Pruning We compare with two model pruning algorithms: the batch-normalization-based pruning (Bn-prune) by Liu et al. (2017) and the L1-based pruning (L1-prune) by Li et al. (2017). Bn-prune imposes L1-sparsity on the channel-wise scaling factors in the batch normalization layers during training, and prunes channels with lower scaling factors afterwards. L1-prune removes the filters with weights of small L1-norm in each layer. For both pruning baselines, we use the implementation provided by Liu et al. (2019b). For Bn-prune, we set the sparsity term to be 0.0001 for all the cases. We initial both pruning methods from a full-size backbone network (MobileNet and VGG19) that we trained starting from scratch. After each pruning phase, the parameters of the pruned network are finetuned starting from the previous values using stochastic gradient descent, following the same setting as that we use in splitting steepest descent.

Finetuning vs. Retraining In both the splitting and pruning methods above, the parameters of the split/pruned networks are successively *finetuned* starting from the previous values. In order to test the performance of the network architectures given by both splitting and pruning methods, we test another setting in which we *retrain* the network parameters after each splitting/pruning step, that is, we discard all the parameters of the network, and retrain the whole network starting from a random initialization, under the network structure obtained from splitting or pruning at each iteration. As shown in Figure 3c-d, the results of retraining is comparable with (or better than) the result of successive finetuning in Figure 3a-b, which is consistent with the findings in Liu et al. (2019b).

B.4 Resource-Efficient Keyword spotting

We apply our methods on the application of keyword spotting. Keyword spotting systems aim to detect a particular set of keywords from a continuous stream of audio, which is typically deployed on a wide range of edge devices with resource constraints.

Dataset and Training Settings We use the Google speech commands benchmark dataset (Warden, 2018) for comparisons. We are interested in the setting that the model size is limited to less than 500K and adopt the optimized architectures with tight resource constraints provided in Zhang et al.

(2017) as our baselines. For fair comparison, we closely follow the experimental settings described in Zhang et al. (2017). We split the dataset into 80/10/10% for training, validation and test, respectively.

We start with a very narrow network and progressively grow it using splitting steepest descent. We build our initial narrow network based on the DS-CNN architecture proposed in Zhang et al. (2017), by reducing the number of channels in each layer to 16. The backbone DS-CNN model consists of one regular convolution layer and five depthwise and pointwise convolution layers (Howard et al., 2017). We refer the reader to Zhang et al. (2017) for more information. At each splitting stage, we increase the number of channels by a percentage of 30% using the approach described in Algorithm 1. We use the same hyper-parameters for training and evaluation as in Zhang et al. (2017).

B.5 Splitting Steepest Descent for Minimizing MMD

We consider the problem of data compression. Given a large set of data points $\{\theta_i^*\}_{i=1}^N$, we want to find a smaller set of points $\{\theta_i\}_{i=1}^n$, equipped with a set of importance weights $\{w_i\}_{i=1}^n$, to approximate the larger dataset. This problem can be solved by minimizing maximum mean discrepancy (MMD) (Gretton et al., 2012) using conditional gradient method (a.k.a. Frank-Wolfe), an algorithm known as *herding* (Chen et al., 2010; Bach et al., 2012). In this section, we provide additional results on using splitting steepest descent to minimize MMD by progressively introducing new points via splitting.

Denote by $\rho_* = \sum_{i=1}^N \delta_{\theta_i^*} / N$ the empirical distribution of the original dataset, and $\rho = \sum_{i=1}^n w_i \delta_{\theta_i}$ the (weighted) empirical distribution of the compressed data. Let $k(\theta, \theta')$ be a positive definite kernel, which can be represented using a random feature expansion of form

$$k(\theta, \theta') = \mathbb{E}_{x \sim \pi} [\sigma(\theta, x) \sigma(\theta', x)],$$

where $\sigma(\theta, x)$ is a feature map indexed by an auxiliary variable x , and π is a distribution on x . The $\sigma(\theta, x)$ can be taken to be the cosine function for commonly used kernels such as RBF kernel; see Rahimi & Recht (2007) for more information on random feature expansion. Then the MMD between ρ and ρ_* , with kernel $k(\theta, \theta')$, can be written into

$$\begin{aligned} \text{MMD}(\rho, \rho_*) &= \mathbb{E}_{\rho, \rho_*} [k(\theta, \theta') - 2k(\theta, \theta'_*) + k(\theta_*, \theta'_*)] \\ &= \mathbb{E}_{x \sim \pi} [(\mathbb{E}_{\theta \sim \rho} [\sigma(\theta, x)] - \mathbb{E}_{\theta_* \sim \rho_*} [\sigma(\theta_*, x)])^2], \end{aligned} \quad (17)$$

where θ, θ' are i.i.d. drawn from ρ and θ_*, θ'_* are i.i.d. drawn from ρ_* . The data compression problem can be viewed as minimizing the MMD:

$$\min_{\rho} \{ \mathcal{L}[\rho] := \text{MMD}(\rho, \rho_*) \}.$$

From (17), this minimization can be viewed as performing least square regression on a one-hidden-layer neural network $f_{\rho}(x) = \mathbb{E}_{\theta \sim \rho} [\sigma(\theta, x)]$, where each data point θ_i is viewed as a neuron. Therefore, splitting steepest descent can be applied to minimize the loss function. This allows us to start with a small number of data points (neurons), and gradually increase the number of points by splitting. The splitting matrix of $\mathcal{L}[\rho]$ is

$$\begin{aligned} S_{\rho}(\theta) &= 2\mathbb{E}_{x \sim \pi} [(\mathbb{E}_{\theta' \sim \rho} [\sigma(\theta', x)] - \mathbb{E}_{\theta_* \sim \rho_*} [\sigma(\theta_*, x)]) \nabla_{\theta\theta}^2 \sigma(\theta, x)] \\ &= 2\mathbb{E}_{\theta' \sim \rho, \theta_* \sim \rho_*} [\nabla_{\theta\theta}^2 k(\theta, \theta') - \nabla_{\theta\theta}^2 k(\theta, \theta_*)]. \end{aligned}$$

We apply splitting steepest descent (`Optimal Split`) in Algorithm 1 starting from a single point (neuron). We compare our method with `Random Split`, `Gradient Boosting` (a.k.a. Frank-Wolfe or herding), `New Initialization`. In `Random Split`, we randomly pick a point to split, and split it following its splitting gradient direction. In `Gradient Boosting`, a new point is introduced greedily at each iteration by minimizing the MMD loss, with all the previous points fixed. In `New Initialization`, a new random point is introduced and co-optimized together with all the previous points at each iteration.

In our experiment, we construct ρ_* by drawing an i.i.d. sample of size $N = 1000$ from a one-dimensional Gaussian mixture model $0.2\mathcal{N}(-2, 0.5) + 0.3\mathcal{N}(1., 0.5) + 0.5\mathcal{N}(3, 0.5)$ as ground truth. We initialize all the methods from a same point drawn from `Uniform`[-5, -3], and add a new point in each splitting/growing phase. The parametric descent phase is performed using the adagrad optimizer with a constant learning rate 0.01 for all the methods.

Figure 7 plots the training dynamics of all the methods. The size of each dot represents the particle weight. Note that in `Optimal Split` and `Random Split`, each off-spring shares half of the weights of their parent points, but in `New Initialization` and `Gradient Boosting`, all the points evenly divide the weights all the time.

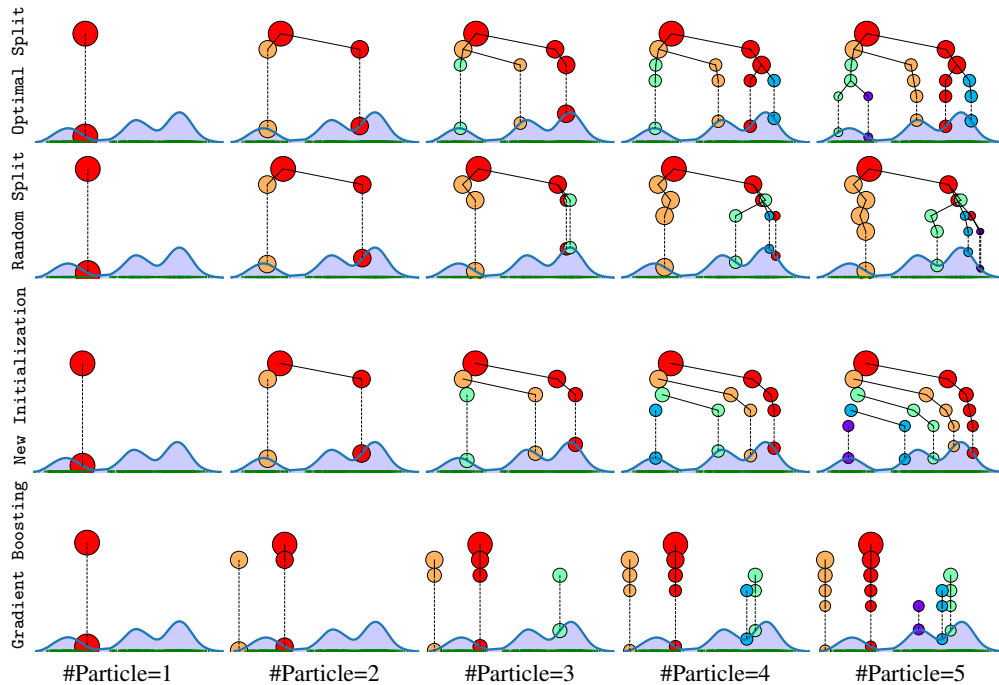


Figure 7: MMD minimization for data compression using different progressive optimization methods.

Figure 8 shows the training iterations vs. the training loss (logarithm of MMD) of our method and the baseline approaches. As we can see from Figure 8, our method yields the lowest training loss in general. The kicks of `New Initialization` and `Gradient Boosting` are resulted from re-weighting all particles after introducing new particles.

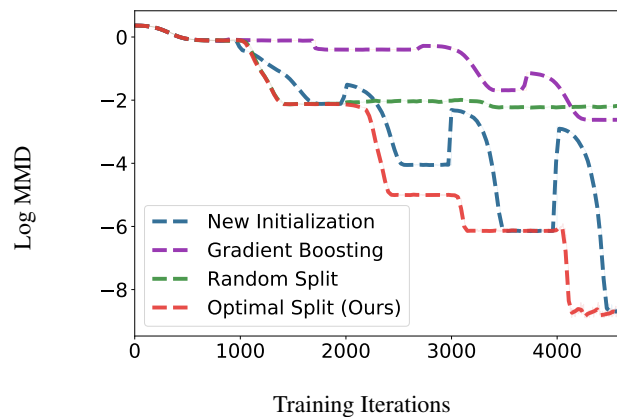


Figure 8: Lose curve of different methods for MMD minimization.